AFWL-TR
65-51

BEHAVIOR OF ROCKS AND SOILS UNDER HIGH PRESSURE

B. W. Paulding
R. H. Cornish
B. W. Abbott
L. A. Finlayson

IIT Research Institute
Chicago, Illinois
Contract AF29(601)-6411

TECHNICAL REPORT NO. AFWL-TR-65-51

December 1965

AIR FORCE WEAPONS LABORATORY
Research and Technology Division
Air Force Systems Command
Kirtland Air Force Base
New Mexico

AFWL-TR-65-51

Research and Technology Division
AIR FORCE WEAPONS LABORATORY
Air Force Systems Command
Kirtland Air Force Base
New Mexico

When U. S. Government drawings, specifications, or other data are used for any purpose other than a definitely related Government procurement operation, the Government thereby incurs no responsibility nor any obligation whatsoever, and the fact that the Government may have formulated, furnished, or in any way supplied the said drawings, specifications, or other data, is not to be regarded by implication or otherwise, as in any manner licensing the holder or any other person or corporation, or conveying any rights or permission to manufacture, use, or sell any patented invention that may in any way be related thereto.

This report is made available for study with the understanding that proprietary interests in and relating thereto will not be impaired. In case of apparent conflict or any other questions between the Government's rights and those of others, notify the Judge Advocate, Air Force Systems Command, Andrews Air Force Base, Washington, D. C. 20331.

Distribution of this document is unlimited.

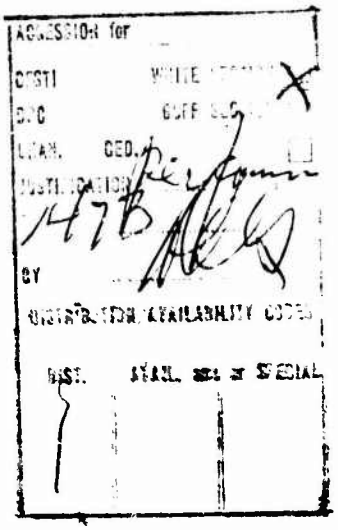

AFWL-TR-65-51

BEHAVIOR OF ROCKS AND SOILS UNDER HIGH PRESSURE

B. W. Paulding

R. H. Cornish

B. W. Abbott

L. A. Finlayson

IIT Research Institute
Chicago, Illinois
Contract AF29(601)-6411

TECHNICAL REPORT NO. AFWL-TR-65-51

FOREWORD

This report was prepared by IIT Research Institute, Chicago, Illinois, under Contract AF29(601)-6411. The research was performed under Program Element 7.60.06.01.D, Project 5710, Subtask 13.144, and funded by Defense Atomic Support Agency (DASA). Inclusive dates of research are 1 June 1964 to 1 August 1965. This report was submitted for publication on 30 November 1965 by the AFWL Project Officer, Captain Joseph J. O'Kobrick (WLDC).

Dr. R. H. Cornish is primarily responsible for the program at IITRI. Other significant contributors to the program include Drs. I. M. Daniel, and B. W. Paulding and Messrs. B. W. Abbott, J. P. Elliott, L. A. Finlayson, T. Nirro, D. Raske and E. T. Weigand.

This report has been reviewed and is approved.

JOSEPH J. O'KOBRICK
Captain USAF
Project Officer

ROBERT E. CRAWFORD
Major USAF
Deputy Chief
Civil Engineering Branch

JOHN W. KODIS
Colonel USAF
Chief, Development Division

ABSTRACT

This report describes a program which was directed toward developing a capability suitable for generating engineering data on the high pressure mechanical properties of geologic materials. To provide the greatest possible contribution, this effort concentrated on three of the most important deficiencies in high pressure experimental technology: (1) development of a system capable of accepting relatively large samples so that more-nearly representative data may be obtained than with the smaller samples used previously, (2) development of a system suitable for monitoring the strains of highly deformable geologic materials, and (3) development of an encapsulating technique for soils.

Each of these objectives was attained to a certain degree. Specimens up to three inches in diameter were subjected to fluid pressures of several kilobars. The deformation of soil was measured with a potentiometric slidewire device. An encapsulating technique was developed for soils which was suitable up to about two kilobars. Further refinements are necessary, but it appears that the more important of the limitations of past studies have been overcome.

CONTENTS

CONTENTS (Cont'd)

LIST OF FIGURES

LIST OF FIGURES (Cont'd)

SECTION I

INTRODUCTION

1. The Role and Status of Experimental Rock and Soil Mechanics

The confident design and performance predictions of excavations and large engineering structures require an exact knowledge of the mechanical properties of the rock and/or soil at, and neighboring, the construction site. Depending upon the structure and its particular function, such properties would include any one or more of the following: linear and bulk elastic moduli, tensile and compressive strengths, fatigue behavior, and creep characteristics. In addition, depending on the function of the facility, it might be required that these properties be known as a function of confining pressure. Furthermore, certain applications may require knowledge of the dynamic properties of the material surrounding the structure. Thus, there is a rather wide spectrum of information required if one considers the problems facing the design engineer.

At present there is a great deal of interest in the design of buried structures capable of withstanding the effects of nuclear blasts. As a result, new demands have been brought to bear on the fields of rock and soil mechanics because of the unique conditions anticipated from weapon effects as contrasted to the more conventional stress conditions associated with common engineering structures. More specifically, the design and performance predictions of such hardened facilities require, among other things, knowledge of the mechanical behavior of rock and soil when subjected to dynamic stresses of several tens of kilobars.

The direct measurement of the engineering properties of rock and soil under conditions simulating those encountered during nuclear blasts is impractical. Therefore, one must concentrate on determining the mechanical properties under obtainable stress conditions and, at the same time, on obtaining an understanding of the mechanics of deformation so that extrapolation to other stress states is possible. This latter point is important and, unfortunately, has not been the philosophy of most previous studies. An objective evaluation of most past investigations reveals that the primary result was the generation of data on the strength and deformation properties of several rock and soil types with little attempt to determine the mechanics of deformation. However, in the case of rock, some of the more recent investigations (refer to Section II) show that certain mechanical properties can be predicted from fundamental considerations of the composition and fabric. This is a major step in the development of rock mechanics as a useful engineering tool and indicates the importance of determining the actual physical phenomena associated with rock deformation. Hopefully, with continued effort in this direction, one may be able to predict from laboratory and field data the mechanical behavior of a rock or soil mass when subjected to the anticipated stress levels.

At this point it is appropriate to consider the capability of past experimental facilities and techniques to explain the paucity of useful engineering data on rock and soil. Three requirements must be met when investigating the mechanical properties of geologic materials: (1) application of a known stress state, preferably uniform, (2) measurement of the resulting deformations and (3) utilization of a sufficiently large specimen size so that meaningful and representative information is obtained. Consideration of each of these requirements explains, in part, the present lack of useful engineering data on the mechanical

properties of rock and soil. For example, prior to the introduction of shaped specimens, all studies of the mechanical properties of rock were performed either on cubes or short circular cylinders.[1,2,3] It is known that the stress state in such specimens is far from uniform[4] and, therefore, the value of the data is questionable. The application of a confining pressure requires that the material be jacketed to prevent the intrusion of the liquid pressure medium. This presents a particular problem with soils and explains, in part, why high-pressure data on soils is lacking.

Strain-gage technology has reached the point where the strains, even in a high-pressure environment, can be measured accurately for most rock types. However, for soils and some rock types which experience large deformations, readily available instrumentation, suitable for high pressure experimentation, is nonexistent.

Regarding specimen size, all previous work on the high pressure behavior of rock has employed specimens of 1/2 to 1 inch in diameter and a few inches long. Therefore the investigator is severely limited since he must restrict his study to rocks of rather fine grain size and with no obvious flaws.

2. Purpose of This Investigation

The primary purpose of this investigation was to develop a facility, consisting of equipment and techniques, which meets the previously mentioned requirements for measuring the mechanical properties of rock and soil. As a result, most of the time expended in this program was directed toward overcoming such fundamental limitations of past studies as the inability to (1) subject large specimens to several kilobars confining pressure;

(2) encapsulate porous and highly deformable materials to prevent the intrusion of the pressure medium; and (3) measure and record the strains of highly deformable materials, such as soil, when the specimen is in a high-pressure environment.

Confronted with these rather unique objectives, the approach used throughout this program has been one of innovation, modification, and occasionally deletion, of equipment and techniques. Several possibilities confront the experimenter at the inception of such a study. Each must be tried until the successful technique is found. The approach in this program manifested itself in the fact that several different techniques were applied toward the attainment of each objective. Specifically, three concepts in slidewire instrumentation, four types of adhesives for strain gage installation, four types of encapsulation, and two methods each of subjecting a specimen to a stress difference, generating high fluid pressures and determining the compressibility of a material were utilized.

3. Outline of Report

Section II of this report contains some theoretical considerations of the mechanical properties of rock and soil. Although not too appropriate, perhaps, for a study concerned mainly with the development of equipment and techniques, the theoretical considerations are presented to acquaint the reader with the present status of rock and soil mechanics and to trigger some thoughts on directions to go in future research efforts. Section III contains a brief description of the geologic materials used in this study. A detailed description of the experimental equipment and techniques is presented in Section IV. The experimental results are presented in Section V. A brief description of a 50 kilobar solid and liquid pressure is presented in Section VI. Section VII contains an objective evaluation of the equipment and techniques developed in this study and suggestions for further refinements toward the attainment of an appropriate high-pressure facility capable of measuring the engineering properties of geologic materials.

SECTION II

THEORETICAL CONSIDERATIONS

An obvious simplification would exist if rock and soil, in general, were ideal elastic materials, that is, homogeneous, isotropic, and linearly elastic (Hookean). If this were the case, only a few laboratory tests would be required to uniquely determine the elastic properties. For example, an ordinary uniaxial compression test could be used to measure E, the modulus of elasticity; and ν , Poisson's ratio. From these two constants the shearing modulus, G , may be determined from

$$G = \frac{E}{2\ (1 + \nu)} , \tag{1}$$

and the bulk compressibility, β , may be found from

$$\beta = \frac{3\ (1 - 2\nu)}{E} . \tag{2}$$

Unfortunately, most rocks and soils do not behave in the manner described above. Their anisotropic nature, due to different mineral constituents, bedding, internal flaws, packing, etc., causes them to behave quite differently than in the purely elastic case. Therefore, for most cases, the simple relations between the elastic constants cannot be applied, and the mechanical properties must be measured directly. The remainder of this section consists of a discussion of mechanical properties of rock and soil to acquaint the reader with the present status of rock and soil mechanics and to trigger some thoughts on the direction of future efforts.

1. Rock

a. Elastic Behavior of Several Common Rocks

The relationships described previously are valid only for materials which exhibit simple elastic behavior, i.e., are isotropic and linearly elastic. There are several common rock types which, particularly at low confining pressures, are decidedly anisotropic and nonlinear. Typical characteristics of such rocks are:

(a) nonlinear pressure versus strain curves obtained during compressibility tests,
(b) nonlinear stress versus strain curves obtained during uniaxial compression tests,
(c) discrepancies between the static and dynamic values of Young's modulus,
(d) rapid changes in sonic velocities with increasing confining pressure, and
(e) variation of Young's modulus, linear compressibility and sonic velocity with direction in a given specimen.

At higher confining pressures, most of the nonlinear characteristics mentioned above disappear.[5,6] However, behavior may still be anisotropic particularly for those rocks which have preferred mineral orientation. Even so, the degree of anisotropy is generally much less than at lower pressures.[5]

A substantial amount of evidence indicates that the characteristics of this pressure-dependent elastic behavior of rock are due to the small, but finite, porosity of natural rocks. For many rock types the porosity is due to transgranular cracks or grain boundary openings. The description and interpretation of several different types of experiments are presented to aid the reader in understanding the importance of cracks on the elastic properties of rock.

(1) Linear and Bulk Compressibility

A plot of pressure versus volumetric strain typical of several rocks is presented in figure 1. At low pressures, the compressibility is high, i.e., there is a large volumetric strain for a small pressure increment. As the pressure is raised the rock becomes stiffer and eventually the curve becomes essentially linear.

This nonlinear behavior is generally attributed to cracks. Walsh[7] made a theoretical study of the effect of cracks on the compressibility of rock. He considered rock to be an elastic isotropic material containing randomly oriented narrow cracks. With this model he derived an expression for the effective compressibility in terms of the compressibility of the solid material and the rate of change of the porosity with external pressure.

He then divided the body into regions, each of which contains one crack. The compressibility of a region after the crack has closed is the same as for the uncracked material. Thus the stiffness of the rock gradually increases as the cracks close under increased confining pressure. For rocks where the entire porosity is caused by cracks which close completely under pressure, the compressibility decreases to the value of the uncracked material.

Brace[6] has shown that the compressibility of the solid material, i.e., the slope of the linear portion of the compressibility curve, agrees within a few percent of the average of the Voight and Reuss values.[8,9] However, it is important to realize, that at the lower pressures, the elastic behavior is mainly controlled by the cracks and not the elastic properties of the solid material.

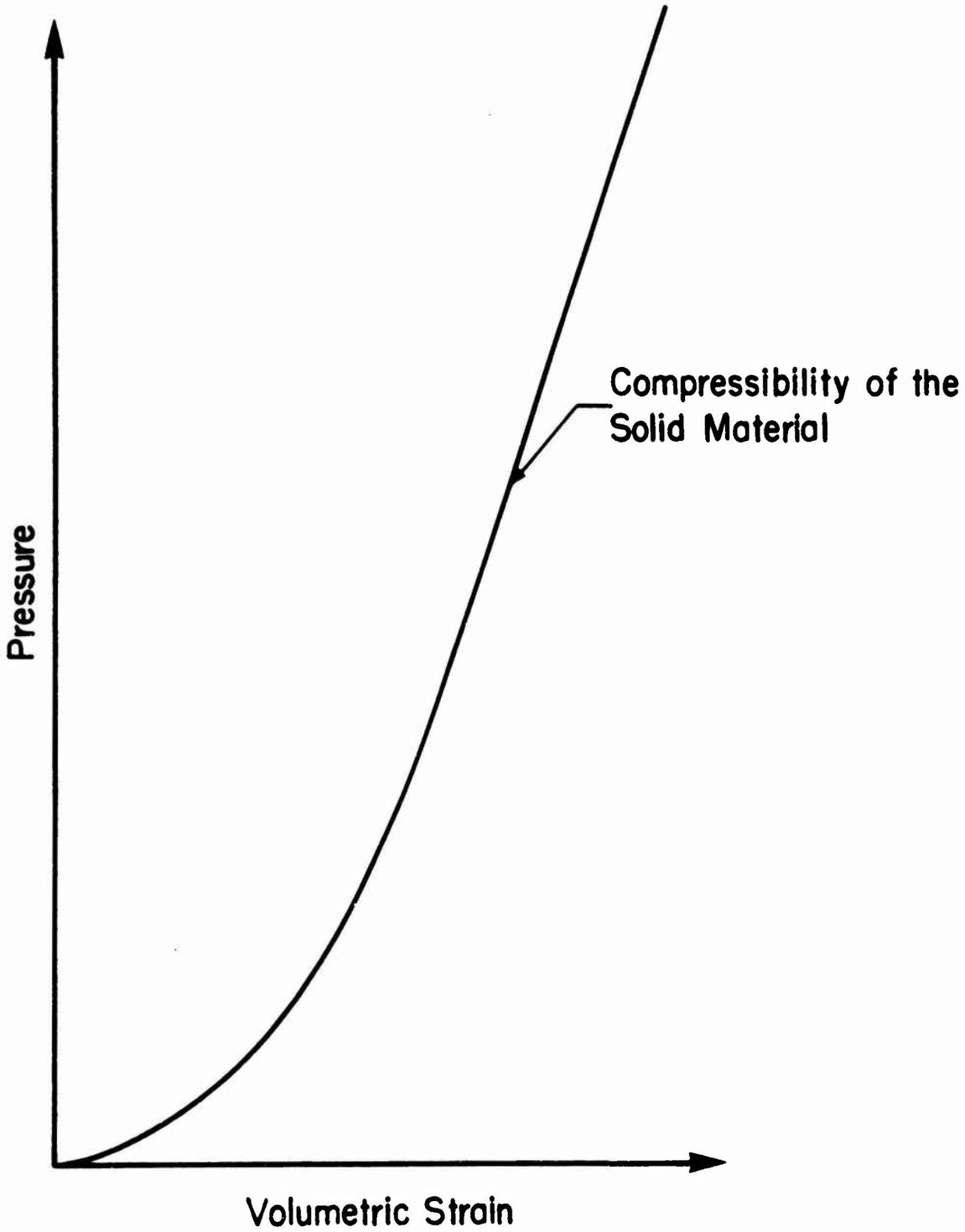

Figure 1. Typical Compressibility Curve of Rock Containing Narrow Cracks

(2) Uniaxial Compression

A stress versus strain curve, typical of those obtained during a uniaxial compression test on common igneous rocks, is shown in figure 2. The nonlinear behavior during the initial stress buildup is characteristic of rocks whose porosity is due to narrow cracks. The low value of Young's modulus, E , is due to the large axial strains at low stress levels which result from the closing of cracks oriented so as to close under the applied stress. As the stress increases, more and more cracks close, resulting in the increasing values of E. Above a certain stress, the stress-strain curve is essentially linear. However, this might not be the intrinsic value of E as predicted from the elastic properties of the component minerals. Walsh[10] has extended his analysis of the effect of cracks on the elastic behavior of rock to include the effect of frictional sliding along the crack walls once they have closed. If this frictional sliding occurs during a uniaxial compression test then the value of E measured from the slope of the ascending portion of the curve would be less than the value predicted from the elastic properties of the solid material.

(3) Static and Dynamic Values of Young's Modulus

It is commonly observed that the static and dynamic values of Young's modulus differ.[11,12] In general, the dynamic values are larger than the static. Walsh[10] has explained this as due tc the effect of the frictional sliding along the crack walls. As mentioned before, where the stress level is above that required to close all the cracks oriented such that they will close under a uniaxial stress, frictional sliding occurs along crack walls and gives a lower value of E than expected from consideration of the elastic properties of the material. This would be the static value of Young's modulus.

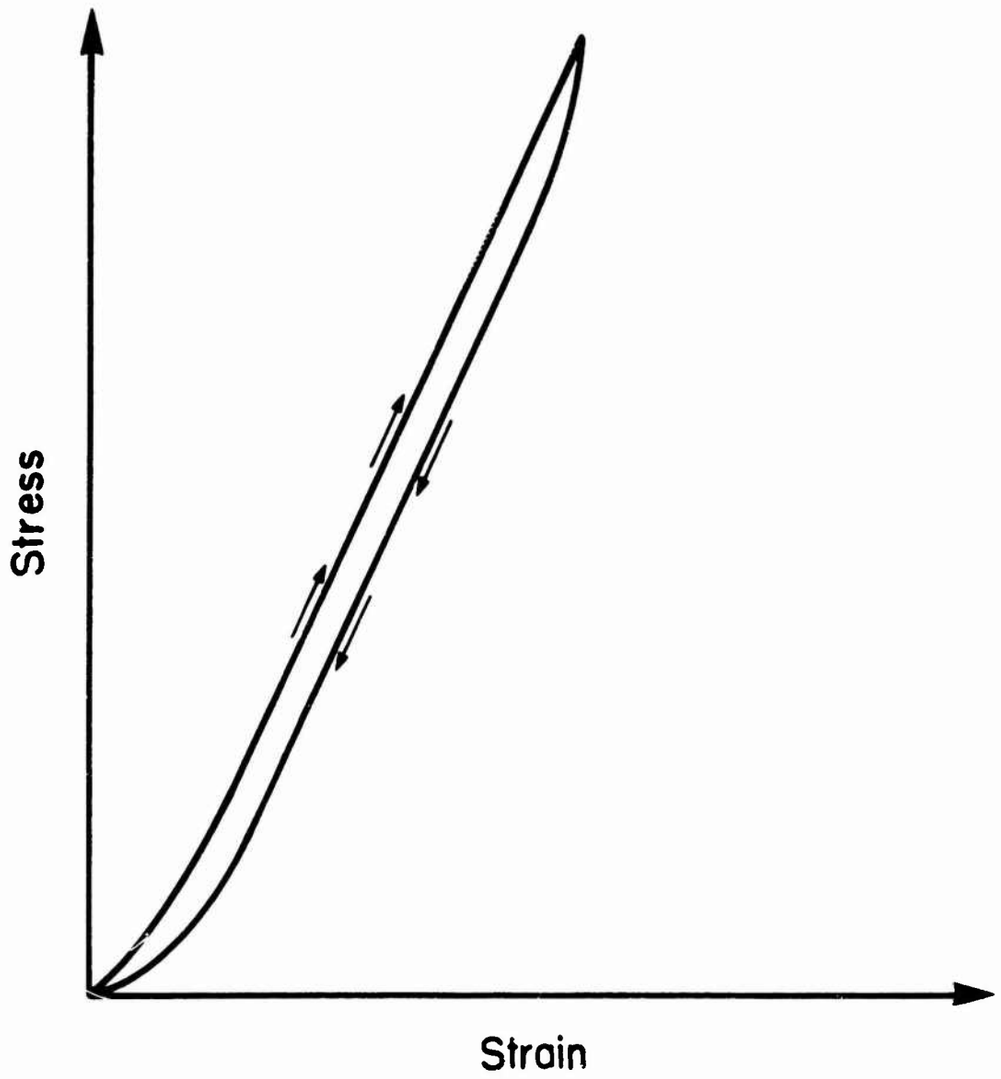

Figure 2. Typical Stress-Strain Curve for Rock Containing Narrow Cracks

If the stress is reduced slightly, the initial slope of the descending portion of the curve is generally found to be greater than the ascending portion over the same stress increment. During a dynamic test, the stress pulse subjects the rock to a small stress cycle. As the pulse first arrives (assume compressional) the strains follow the ascending portion of the curve. As the stress pulse passes the point in question, the strains follow the descending portion of the curve. The value of E as determined from sonic velocities, then, is the average of the ascending and descending portions of the curve at the stress interval at which the test was conducted.

(4) Dependence of Sonic Velocity on Confining Pressure

Another example of the effect of narrow cracks on the elastic properties of rock is the increase of sonic velocities with increasing confining pressure such as reported by Birch.[5] As Birch stated, the increase in velocity with increasing confining pressure resulted from the reduction in porosity due to the closing of cracks.

(5) Variation of Elastic Properties With Direction

Rocks with an obvious fabric orientation, for example, gneisses, schists, and shales, have elastic properties which, as expected, are strongly dependent on the direction in which the measurement is made. Examples of this are the sonic velocities reported by Birch.[5]

Other rocks, which do not have an obvious foliation or mineral orientation, also show anisotropic elastic behavior. Brace reported linear compressibilities for several rocks.[6] One, a granite, showed marked anisotropy at the lower pressures. Apparently, this was due to a preferred direction of either grain boundaries[6] or transgranular cracks.[2]

It is only natural to consider the effect of cracks on the elastic properties of rock subjected to a confining pressure. From the compressibility tests one sees that the cracks have closed once the hydrostatic pressure reaches a certain level, generally a few kilobars.[6,7] The natural question is, once cracks have closed, can we expect the above-mentioned ideal elastic relationships to be valid?

Some insight into the behavior of cracks once they have closed is provided by the analysis of McClintock and Walsh.[13] They modified the Griffith theory of fracture[14,15] by considering the effect of frictional stresses along the crack walls on the stress concentration factor of a crack. Agreement was found between their analysis and the onset of crack growth.[2] Walsh[10] has recently studied the effect of cracks on the uniaxial elastic properties of rock and determined the coefficient of friction along crack walls with data taken from uniaxial stress versus strain curves. The significance is that for the same rock type, Walsh determined a coefficient of friction of 0.65 ± 0.05 from the uniaxial data and Paulding found a value of 0.7 ± 0.10 from triaxial data.[2]

Another characteristic common to several rock types is the hysteresis loop associated with uniaxial tests even though the rock has been cycled to only a small fraction of its fracture strength. A typical curve is shown in figure 2. This phenomenon has been explained as being due to the frictional sliding along cracks.[10] As the stress is raised, grains or portions of grains tend to slide past one another. Sliding in the reverse direction does not occur until the stress is at a lower level than that where the initial sliding took place. This results in the large strains at the same stress level on the return curve as shown in figure 2.

Therefore, even though cracks may be closed due to the application of a confining pressure, there is evidence that frictional sliding can still occur when the rock is subjected to a deviatoric stress. This then suggests that, at intermediate confining pressures, the cracks can influence the deformational properties of rock and that the agreement with the ideal elastic relationships may not exist.

As mentioned before, the coefficient of friction along crack walls was found to be about 0.7. This value appears reasonable when compared with values obtained from direct measurements; Handin,[16] Paterson,[17] and Jaeger[18] have independently reported values of the coefficient of friction of rock on rock which range from 0.4 to 0.9.

The existence of a coefficient of friction of nearly unity suggests that a substantial deviatoric stress may be borne at the higher confining pressures without the associated frictional sliding along the crack walls. This, in turn, suggests that the higher the confining pressure, the greater will be the stress difference required to cause frictional sliding. Therefore, at these higher confining pressures the elastic properties of several rock types may be related in a manner not too different from that of the elastic constants of an elastically ideal material.

b. Strength Properties

Experimental data obtained from fracture studies are most commonly compared with the predictions of two failure criteria: (1) the Navier-Coulomb (a modification of Mohr's theory), and (2) the Griffith theory (or theories based on Griffith's model such as the McClintock-Walsh modification of the Griffith theory).

The Navier-Coulomb theory is appealing because it appears to explain why the failure plane in a compression specimen is inclined to the direction of maximum compression. Coulomb stated[19,20] that failure occurs along a plane when the shear stress becomes equal to the shear strength of the material. This theory predicts that (1) the failure plane is inclined at 45 degrees to the direction of maximum compression and (2) the tensile and compressive strengths are equal. However, failure planes are generally observed to be less than 45 degrees from the direction of maximum compression and the tensile strength is generally found to be a small fraction of the compressive strength.[19]

These difficulties were removed by Navier[19,20] who modified Coulomb's theory by assuming that the shear strength of the material is increased by a constant, μ , times the normal pressure across the plane. The constant, μ , is commonly called the coefficient of internal friction. If σ and τ are the normal and shear stress across a plane, the Navier-Coulomb criterion states that fracture occurs when the shear stress equals the sum of the shear strength of the material, S_o , and the frictional stress, $\mu\sigma$.

Brace[21] pointed out a fundamental inconsistency in the Navier-Coulomb theory by questioning the simultaneous existence of a shear strength and a frictional stress at a point in the material. Paulding[2] pointed out an additional difficulty by obtaining partially fractured specimens and noting that permanent slip had occurred along a fracture plane which extended only part way through the sample. This suggested that even if the discrepancy noted by Brace were accounted for, the theory should be further modified to allow for the fact that the entire fracture plane does not form instantaneously. Even though the Navier-Coulomb theory is beset with these difficulties, it is found that qualitative agreement usually exists between the theory and fracture data from triaxial tests.[19]

Most of the recent work on the fracture mechanics of rock has been concerned with determining the applicability of the Griffith theory of brittle fracture.[14,15] Griffith was the first to point out the stress concentrating effect of cracks or flaws in a material. Using Inglis' elastic solution[22] of the stress state around elliptical openings, Griffith derived an energy balance which stated that the crack would propagate when the decrease in strain energy was sufficient to provide the energy of the newly formed surfaces. Griffith's equation for the tensile strength of a material is:

$$T_o = \sqrt{\frac{E\gamma}{\pi C}}$$

where

T_o = tensile strength
E = Young's Modulus of material
γ = surface energy of material
$2C$ = crack length.

Griffith then extended his theory to a general stress state and assumed that crack propagation (and therefore fracture) occurred where the local stress near the end of the most critically stressed crack was the same as in the uniaxial tensile case.

Griffith's theory was found to predict lower strengths than found in triaxial tests. McClintock and Walsh accounted for this discrepancy by modifying Griffith's analysis to include the closing of cracks during the application of a confining pressure.[13] The frictional stress which exists once a crack has closed tends to resist any additional deformation of the crack and therefore the crack is less likely to propagate. Their analysis predicts the confined compressive strength in terms of uniaxial compressive strength, confining pressure and the coefficient of friction along the crack walls. Agreement was found with the results of several investigators if the coefficient of friction was taken to unity.

However, it was recently found that crack growth occurs in several common rock types at stress levels much less than the compressive strength.[2] Since the Griffith model predicts failure when the most severely stressed crack propagates, it was concluded that neither the Griffith theory nor the McClintock-Walsh modification can be expected to predict the compressive strength of rocks.[2]

Even though Griffith's theory does not predict the compressive strength of materials, there is a substantial amount of evidence which indicates that naturally occurring cracks in rock have a pronounced effect on the strength. Brace[23] found that the compressive strength of certain rocks was dependent on maximum grain size. By considering grain boundaries as "Griffith cracks", he found that the compressive strength depended on the crack length as predicted by Griffith. The effect of an anisotropic crack pattern on the compressive strength was studied by Walsh and Brace.[24] They found fairly good agreement between their theory and the results reported by Donath[25] on oriented cylinders of shale and slate.

Thus, it is apparent that cracks have a pronounced effect on the strength of rock and as with elastic properties, it is important that their effect be considered.

The preceding section briefly outlined some of the most recent findings of deformation studies on rock. Since the effect of cracks and flaws on the mechanical properties of rock is important, the logical question is: "How can one predict the mechanical properties of large masses of rock with which the mining or civil engineer must deal?" In these situations, the rock mass may incorporate several different rock types, each with their own mechanical properties, and major discontinuities such as joints, bedding and faults. It would be convenient if laboratory data could be extrapolated to field dimensions. Unfortunately, this stage of development has not been reached.

A basic requirement enabling the attainment of this status is to extend present knowledge by studying samples with large flaws. The effects of cracks on the mechanical properties described earlier were all obtained from samples no larger than 1 inch in diameter and a few inches long. All of the samples (with the exception of Donath's) were chosen because they appeared, megascopically, as uniform material with very small flaws (generally no larger than the grain size). An important, necessary step is to study the mechanical properties of larger samples which contain flaws visible to the naked eye, for example, cleavage. Data obtained from such samples could then be compared with data obtained from samples with small flaws. This would allow one to see if it is possible to extrapolate, at least over this size range, with the existing theories, and if not, how these theories should be modified.

2. Soil

Rather than summarize the extensive work of the past several decades on the mechanical properties of soil, this particular section is devoted to describing some thoughts about a few of the existing concepts of soil behavior and their merit, particularly at high confining pressures. This is believed to be an appropriate endeavor in view of the fact that the anticipated pressure levels employed in this study far exceed those which past tests have utilized, and thus require a fresh look at some of the generally accepted concepts obtained largely from tests at low confining pressures. It is felt that soil mechanics will continue to remain an empirical science unless considerations such as those presented below are exercised. Without a fundamental understanding of what is actually happening during the deformation of soils, with the goal of developing a valid model of the physics of deformation, one is severely limited in the confident extrapolation of laboratory data to predict the mechanical properties of soils under conditions not obtainable in the laboratory.

To best present the considerations given to soils under high confining pressures, two types of experiments will be described: (1) hydrostatic compression of a noncohesive soil and (2) triaxial compression of a cohesive soil.

a. Hydrostatic Compression of a Noncohesive Soil

Consider a jacketed sample of a partially saturated sand, in a slightly open-packed condition which is subjected to an increasing hydrostatic pressure. Imagine that the test is "nondrained," that is, the fluid pressures are allowed to increase once the porosity is reduced to the point at which the material becomes fully saturated. As the pressure is raised initially, there will probably be a rather pronounced decrease in volume as the particles rearrange to a more dense packing. With further increases in pressure the slope of the pressure versus volumetric strain curve may become nearly linear as the grains undergo elastic deformation. At higher pressures the volume may decrease more rapidly as the high contact stresses cause some of the grains to fracture, resulting in the filling of some of the available voids. Imagine that the sample is now completely saturated. At this point, the pore fluid pressures will increase such that some of the additional applied pressure increments will be borne by the pressure. The common assumption is that once a soil is completely saturated, all additional applied pressure increments are completely borne by the pore fluids and that the effective stress, i.e., the grain to grain contact stress, remains constant. However, at higher pressures (of the order of kilobars) this reasoning may not be valid since the relative compressibilities of the pore fluid and grains must be taken into account. At high pressures it might be expected that the volume decrease of the sample will be the result of continued elastic deformation and fracturing of the grains and the compressibility of the pore fluid.

b. Triaxial Compression of Cohesive Soil

It is generally accepted that the Navier-Coulomb failure model is best suited for predicting the strength characteristics of soils. However, it is instructive to look closer at the model. Briefly, it states that the resistance to sliding along a potential shear surface is made up of a cohesion term and a frictional term which act simultaneously along the given plane. There appears to be a fundamental inconsistency in this reasoning.[21] Consideration of the situation at any point along the potential shear plane will clarify this inconsistency. If the point happens to lie within a particle, then the lack of any free surface precludes the presence of any frictional term and the resistance to shear at such a point would be provided by the shear strength of the particle. Imagine, next, that the point lies at the point of contact of two grains or clay platelets. Here, the resistance to sliding would be provided by friction without any cohesive term dependent on the cohesive strength of the particles.

Furthermore, it has been found for such brittle materials as rock, that the entire fracture surface is not formed simultaneously.[2] Presumably, the same could be true for soils. If so, it would mean that frictional sliding occurred along a plane which passes only partly through the sample and the remainder of the sample is essentially undisturbed. This phenomenon would lead one to seriously question the simultaneous existence of a cohesion term and a friction term along the entire shear plane.

Another phenomenon which the Navier-Coulomb model fails to mention is the effect of the dilatency, i.e., volume increase, which certain soils experience during failure. It has been found that several rock types are dilatent during fracture and that an appreciable amount of the work required to fracture a specimen is expended against the confining pressure medium.[2] It would seem that a valid failure criterion for soils should include this effect of volume increases on the stress difference required for failure.

At higher pressures other factors may enter into the strength of soils which are not normally considered in tests at lower confining pressures. One of these, as explained earlier, is the increase in the effective stress which may occur due to the finite compressibility of the pore fluid. The other factor is the influence of pressure on the coefficient of friction. Without information on measured values of the coefficient of friction of soils as a function of pressure, it is admittedly, conjecture to predict the strength characteristics of soils at high pressures. However, measurements of friction of rock on rock show that the coefficient of friction actually decreases with increasing normal pressure.[16] A similar study should be conducted on soils to determine if there is a similar influence on the coefficient of friction between soil particles. If there is, then the actual strength of soils at high confining pressures might be less than predicted from extrapolation of the data obtained from tests at low confining pressures.

SECTION III

DESCRIPTION OF MATERIALS

Diorite, granite, limestone, sand and clay were chosen as typical common rock and soil samples. The following are descriptions of the materials used in this study. The mineralogy and volume percentages were obtained from examination of hand specimens. The specific gravity was determined from samples exposed to normal laboratory conditions of temperature and humidity.

Grey Hornblende Quartz Diorite

Specific Gravity = 2.74
Grain Size: Range, 1/2 to 6 mm; Average: 1.5 mm

Mineralogy	Approximate Volume Percentage
Plagioclase	65
Hornblende	20
Quartz	10
Biotite	5

Grey Biotite Granite

Specific Gravity = 2.65
Grain Size: Range, 1/2 to 4 mm; Average: 1 mm

Mineralogy	Approximate Volume Percentage
Orthoclase	75
Quartz	20
Biotite	4
Muscovite	1

Grey Argillaceous Limestone

Specific Gravity = 2.59

This rock is an impure limestone containing thin, dark, irregular laminae and occasional calcareous inclusions of up to 5 mm in diameter. Sample cores were cut normal to the lamination.

20-40 Ottawa Sand

Specific Gravity = 2.65

Particle Size = 98 percent between 0.84 mm and 0.42 mm

Mineral Content = Better than 99 percent SiO_2, remainder is clay

The particles are well-rounded and off-white.

Clay

Composition: 99 percent kaolinite

Color: White

Generally mixed with water to a water content of about 30-40 percent before testing.

SECTION IV

EQUIPMENT AND TECHNIQUES

1. Stress Application

a. Pressure Vessel

The pressure vessel and pressure-generating equipment used in this study are shown in figures 3 and 4. The vessel itself has an inner diameter and length of 4 and 36 inches, respectively. Since a 3 inch plug is used as a seal at each end, the maximum working length is 30 inches. Each seal plug consists of an O-ring and a brass back-up ring. The seal plug at the bottom of the vessel contains the pressure inlet port where fluid is introduced into the vessel. The top seal, pictured in figure 4, also contains a pressure inlet port and, in addition, a high pressure electrical lead-in system.[26] The electrical lead-in plug contains 28 electrical leads which terminate in a standard Amphenol electrical connection.

The pressure vessel closure procedure is as follows: the top plug is fitted into the bore of the vessel and the two end plates, shown in figure 3, are placed on top of the seal plug. The end plates are then bolted to the vertical tie-bars which are located around the perimeter of the vessel.

Removal of the top plug often required that two bolts be advanced through tapped holes in the top seal so as to butt against the top of the vessel itself. Frequently, however, the top seal could be loosened by merely removing the end plates and then generating a few hundred psi fluid pressure.

b. Pressure Measuring and Generating Equipment

Up to 100,000 psi the pressure was measured with a Heise bourdon tube pressure gage. Beyond this limit a calibrated manganin wire coil was used to monitor the pressure. The pressure

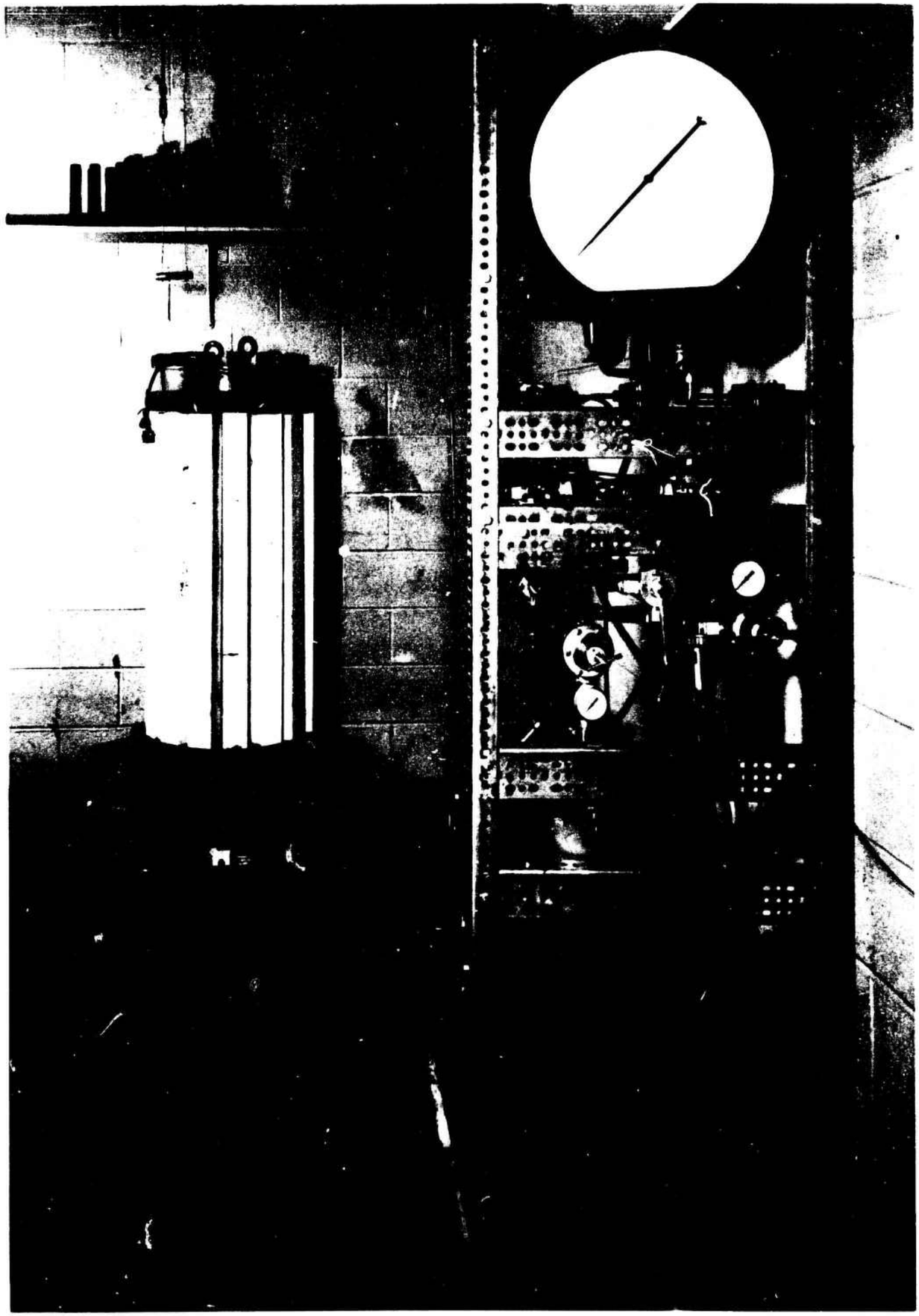

Figure 3. High Pressure Facility

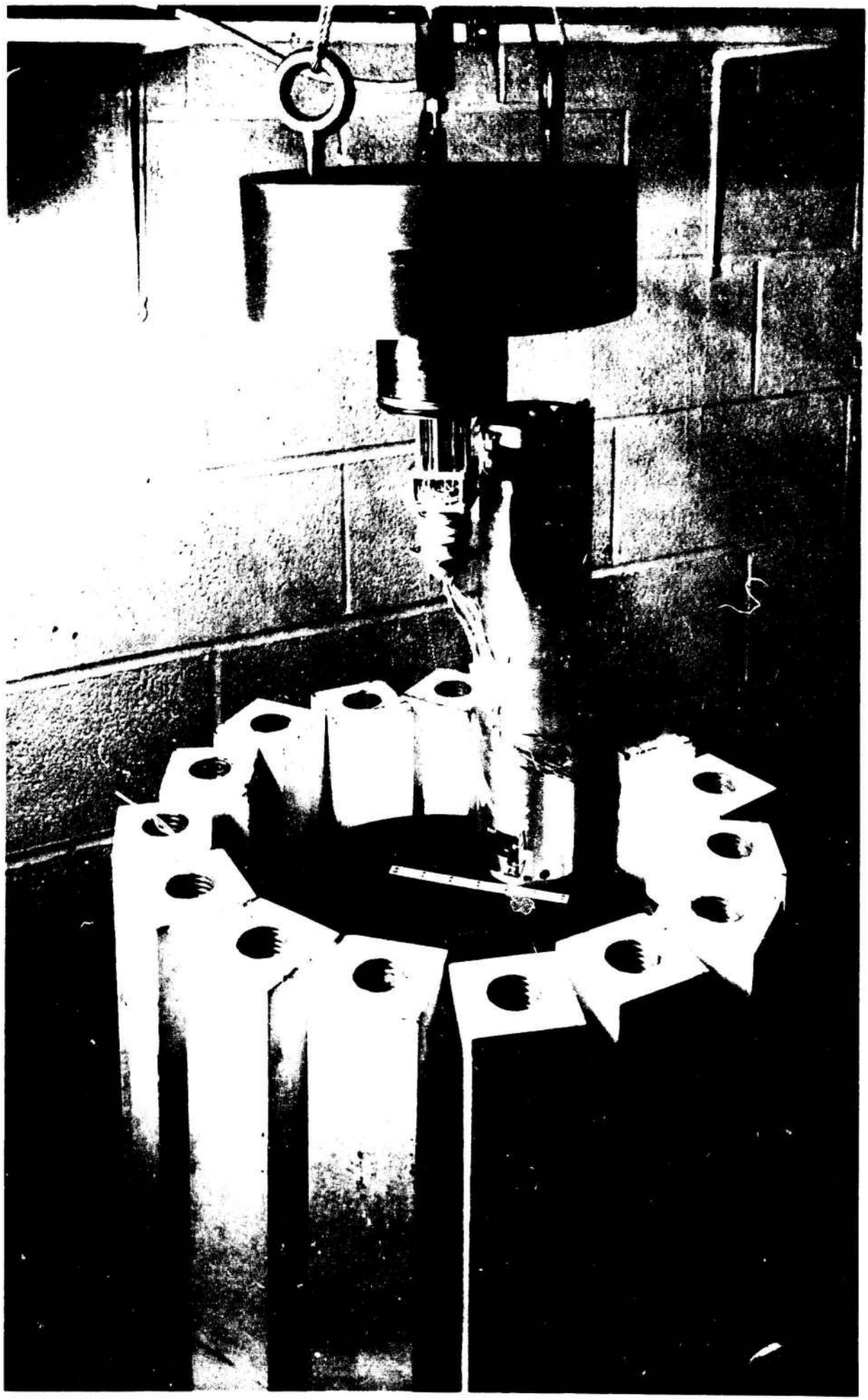

Figure 4. Pressure Vessel

transmitting fluid was a low viscosity silicone oil (100 centipoise at room conditions) manufactured by Dow-Corning Corp. All high pressure fittings, valves and stainless steel tubing are commercially available and are rated for 100,000 psi.

A series of two air pumps and a differential area pressure intensifier were used to generate the high fluid pressures. The pressure generation procedure was as follows: the fluid pressure was increased to 3000 psi by means of a pump (Sprague Engineering Company) activated with air at a pressure of about 80 psi. At 3000 psi, another air pump (Haskel Company) was used to pump the fluid up to a pressure of about 70,000 psi. The Haskel pump was activated by air compressed to about 150 psi. The attainment of pressures greater than approximately 70,000 psi required utilization of a differential area pressure intensifier. The low pressure end of the intensifier was pressured by the Sprague 3000 psi system. Since the area of the piston on the low pressure side was 50 times larger than the area on the high pressure side it was, theoretically, possible to reach 150,000 psi fluid pressures on the high pressure side. However, this pressure level was not attained with the intensifier system. The common problem was reoccurring damage to the pressure seals around the moving piston. This difficulty is discussed further in Section VII.

The second pressure generating system employed in this study consisted of the same components as described above except that a modified air-driven oil pump was used for generating pressures above 60,000 psi instead of the differential area pressure intensifier. This high pressure pump was modified as described by Whalley and Lavergne.[31] They found it suitable for generating 45 cu cm up to 10 kilobars pressure. Although this volume is some hundred times less that the capacity of the vessel employed in this study it was decided to determine its suitability for generating high pressures in a large volume.

Several attempts were made to generate 10 kilobars pressure in the large vessel with this pump. However, the highest pressure obtained was 87,000 psi. The pump functioned properly for a limited number of strokes but then the test had to be discontinued because of damage to the O-ring and back up rings around the moving piston.

c. Bulk Compressibility Apparatus

The fixture that was used for determining the bulk compressibility of the rock and soil specimens is shown in figures 4 and 5. Essentially it consists of a hollow cylinder which contains a sealed piston locked in place at mid-height of the tube. Moving pistons at each end of the fixture complete the dual chamber arrangement. Each end piston contains two O-ring seals as shown in figure 5. A sectional view, illustrating the internal arrangement of the specimens and pistons, is shown in figure 6.

Identically sized specimens are placed on either side of the fixed central block. One of the specimens is of a known compressibility such as steel, while the other sample is of a material whose compressibility is to be determined. Both moving pistons are positioned and the remainder of both chambers are filled (through a port not shown on the drawing) with fluid so that the system is free of voids. The entire apparatus is placed in the bore of the pressure chamber and the vessel is sealed. As the pressure in the chamber is increased, the pistons move so as to equalize the pressure throughout the system. The difference in measured piston displacements represents relative volume change between the known and unknown materials. Hence the compressibility measurement is relative to an established value. In cases where the compressibility and original volume of the fluid in each chamber is known, the absolute compressibility of each of two specimens can be determined simultaneously.

Figure 5. Bulk Compressibility Apparatus

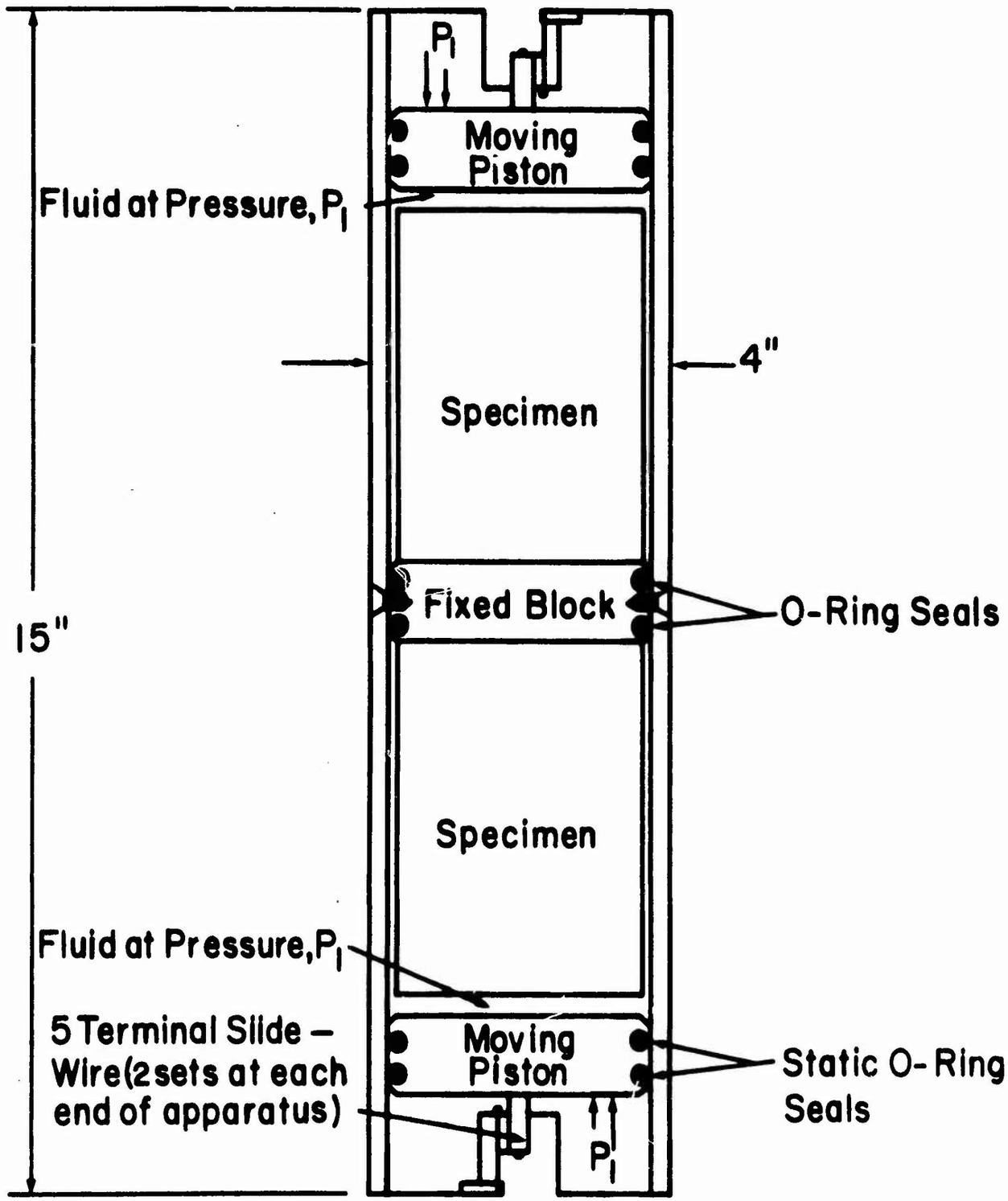

Figure 6. Cross-Sectional View of Compressibility Apparatus (See Also Figures 3,4,5,7,8,9, etc.)

A close-up view of one end of the compressibility apparatus is presented in figure 7 to show the construction detail of the slidewire element which monitors the displacement of the piston. The theory and construction of the slidewire elements will be presented in a later section.

d. Confined Compression Apparatus

The confined compression apparatus used in this study is designed to apply an axial compressive load to a cylindrical specimen which is subjected to a lateral confining pressure. A cross-sectional view of the fixture is shown in figure 8. The specimen is placed in the compression chamber and the moving piston is installed. The screw cap (containing a pressure inlet port) is used to close the chamber. Next the entire unit is sealed in the bore of the pressure vessel. An independent hydraulic line is then run from a pressure source to the pressure inlet port in the top of the fixture.

Confined compression tests are conducted by first increasing the pressure, P_1 , in the vessel through the pressure inlet port in the bottom seal. This subjects the sample to a state of hydrostatic stress. The axial stress in the specimen is then increased by raising the pressure, P_2 , above the moving piston of the compression apparatus.

The force applied to the specimen, F , is

$$F = A_p (P_2 - P_1) - f(P_1)$$

where P_1 = lateral confining pressure
P_2 = pressure above the moving piston
A_p = cross-sectional area of the moving piston
$f(P_1)$ = frictional force at the piston's O-rings.

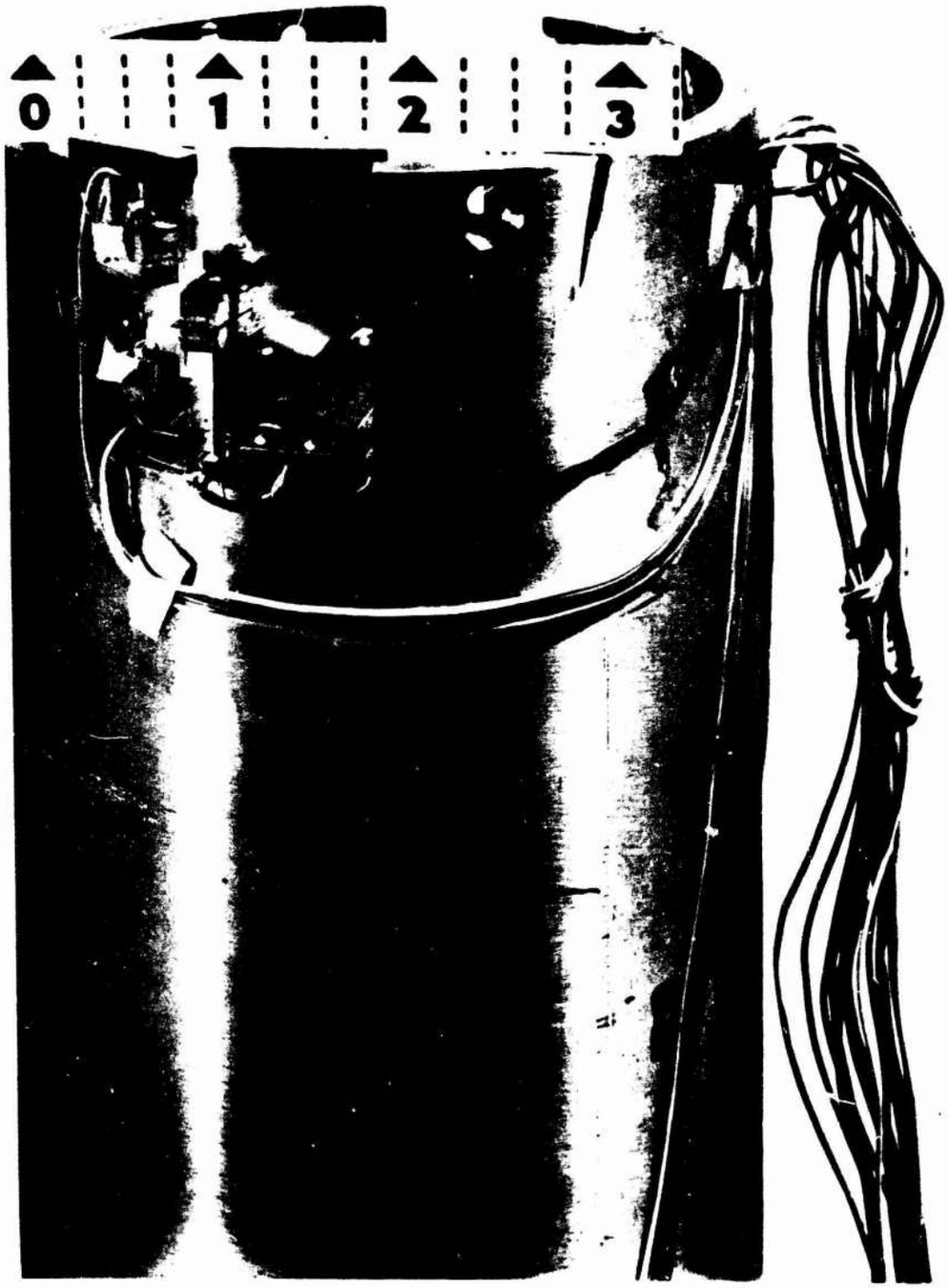

Figure 7. Detail of Slidewire Element of Bulk Compressibility Apparatus

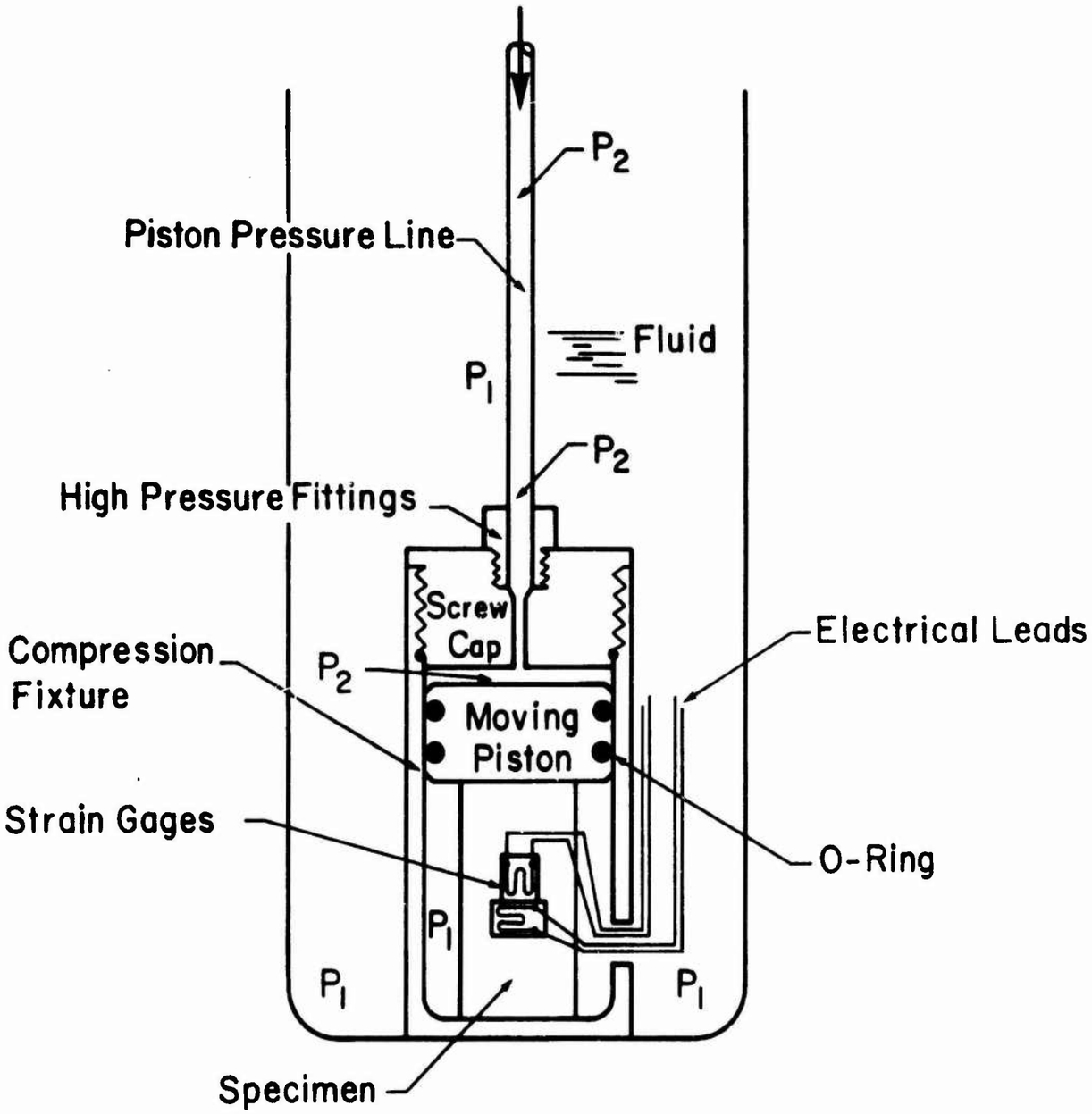

Figure 8. Instrumentation of Confined Compression Tests

The axial stress, σ , in the sample is

$$\sigma = \frac{A_p}{A_s} (P_2 - P_1) - \frac{f(P_1)}{A_s}$$

where A_s = cross-sectional area of the specimen.

The frictional force at the pistons O-rings was found by filling the chamber with oil and then measuring the pressure required to move the piston while monitoring the pressure in the chamber. The following values were found:

for $0 < P_1 < 2500$ psi $\quad f(P_1) = 0$
for $2500 < P_1 < 100{,}000$ psi $\quad f(P_1) = 600$ lb per 10,000 psi.

Figures 9 and 10 are photographs of the compression fixture with suitably instrumented test specimens. In both figures the details of the apparatus are clearly shown. Figure 9 includes a rock specimen which has been instrumented with strain gages. In figure 10 a steel specimen instrumented with both strain gages and slidewires is shown. The electrical leads from these transducers are led out through a hole in the side of the confined compression apparatus and attached to the electrical lead-out plug in the pressure vessel.

e. Torsional Apparatus

A torsional fixture was designed and fabricated to measure the torsional moduli of rock. Its use was restricted to room pressure tests since a suitable encapsulating system for the complex shaped specimens was not developed. Had tests been conducted, the fixture was designed to be assembled as shown in figure 11.

The fixture is designed to accept hollow cylindrical specimens prepared with turret shaped ends which fit the mating grip blocks. In a typical experiment, the specimen would be assembled

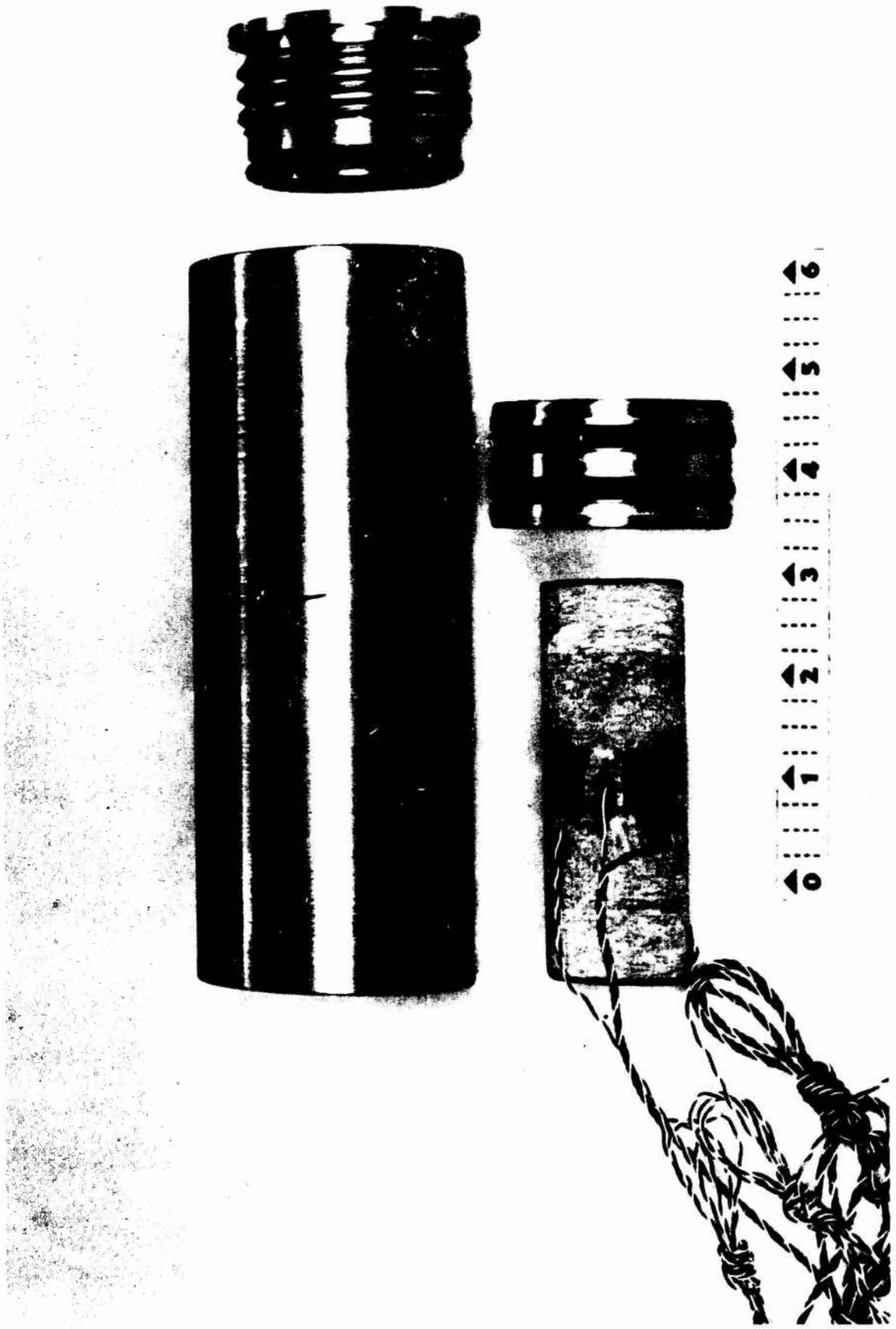

Figure 9. Confined Compression Fixture

Figure 10. Confined Compression Fixture

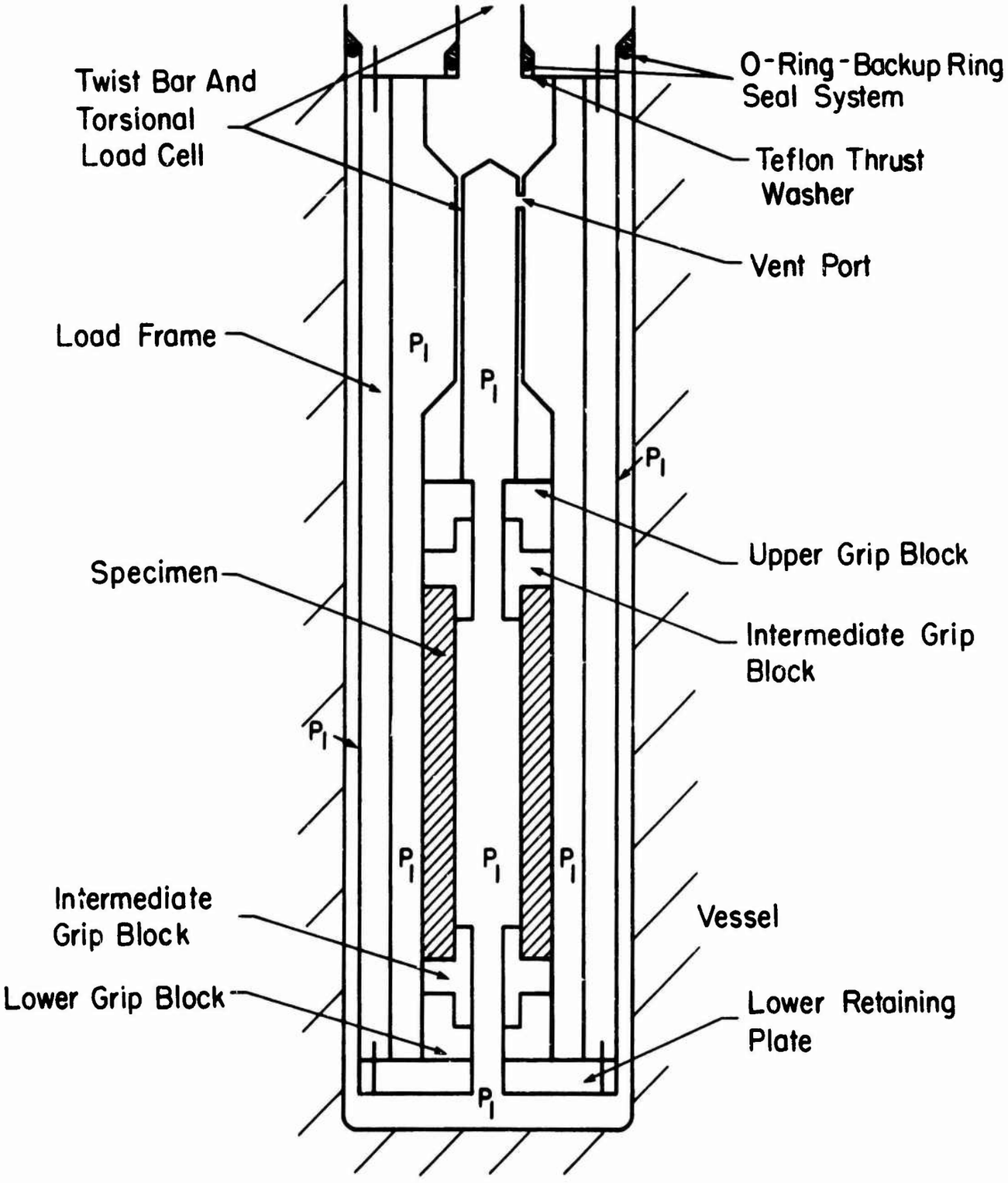

Figure 11. Schematic View of Torsion Test

into the grip blocks which, in turn, are fitted into the torque bar load cell unit at the top of the specimen, and bolted to the fixed load frame at the bottom of the specimen. At any pressure level, P_1 , the entire specimen would experience a hydrostatic state of stress. When a torque is superimposed, a stress difference would be developed throughout the specimen. By measuring the torque and the resulting deformation under these conditions, the torsional moduli of the rock would be determined as a function of the confining pressure.

Figure 12 shows the torsional apparatus in the disassembled condition. The items in the upper portion of the photograph are the vessel seal plug, load frame and lower retaining plate. The upper and lower grip blocks, a typical torsion specimen, and the torque bar load cell are shown in the lower half of the photograph. The load cell is instrumented with strain gages mounted so as to coincide with the principal stress directions. The output of these strain gages, then, would monitor the torque applied to the specimen.

2. Strain Measurement

a. Strain Gage Instrumentation

Electrical resistance strain gages were used as one type of transducer in this study. Most of the gages employed are designated as CX-121 (Budd Instrument Division, Baldwin-Lima-Hamilton Corp.) which is an epoxy backed etched foil gage having a 1/8 inch square grid and a resistance of 120 ohms. The strain gages were mounted directly to the specimen surfaces with any one of several different types of cements: cyanoacrylate monomer contact cement (Eastman 910, Budd Company), a room temperature-elevated temperature cure epoxy cement (type RTC, William T. Bean, Inc.), and an elevated temperature cure epoxy (Araldite, Ciba Products Corp.) were used. Following installation, vinyl plastic, modified silicone resin and rubberized epoxy encapsulating materials were applied over the gages to protect them during handling. Figure 13 is a photograph of two typical specimens instrumented in this manner.

Figure 13. Specimens Instrumented with Strain Gages

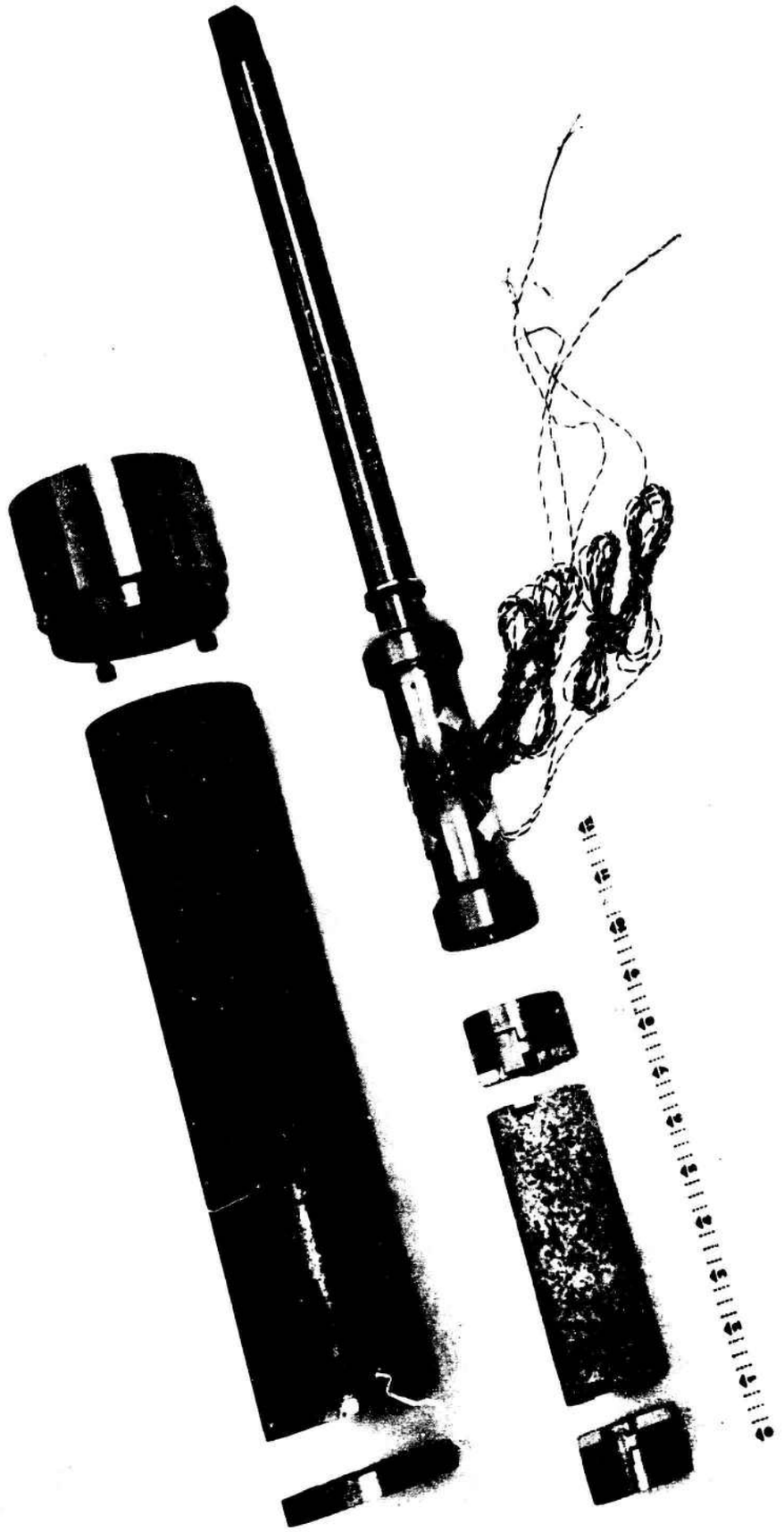

Figure 12. Torsion Apparatus

The apparent simplicity of using electrical resistance type strain gages is appealing but the successful use of such under high fluid pressures required consideration of several important factors. It is known that there is a pressure effect on strain gages at high pressure.[27,28,29,30] In some instances, this effect is of sufficient magnitude that it must be accounted for if the actual strains are to be determined accurately. Secondly, the electrical lead-out wires, which in this case are swaged thermocouple wires, undergo substantial resistance changes as a function of pressure. Unless the effect of resistance changes of the lead-out wires is eliminated, the measured strains will be erroneous.

A direct current potentiometric circuit was employed to avoid the effects of changes in resistance of the swaged thermocouple wires. In this circuit the voltages on a standard (dummy) gage, active gage combination, were read in succession and the net strain was computed from the measured voltages. The circuit is illustrated diagrammatically in figure 14. Successive voltage readings of A_1B_1, C_1V ; A_2B_2, C_2V; etc., provide the input data from which the strains are calculated. The pressure-induced resistance changes of the swaged thermocouple wire from the active gages are not measured since the potentiometric circuit draws no current at balance.

Since the current, I , is the same through each standard-active gage combination, the ratio of the voltages across each gage is equal to the ratio of the resistances:

$$\frac{V_{go}}{V_{so}} = \frac{I\ (R_{go})}{I\ (R_{so})} = \frac{R_{go}}{R_{so}} ,$$

where V_{go} = original active gage voltage
V_{so} = original standard gage voltage
R_{go} = original active gage resistance
R_{so} = original standard gage resistance.

Figure 14. Potentiometric Strain Gage Circuit

Since

$$R_{go} = R_{so} \left(\frac{V_{go}}{V_{so}}\right)$$

then, at constant temperature,

$$\Delta R_g = R_{so} \left(\frac{V_{gn}}{V_{sn}} - \frac{V_{go}}{V_{so}}\right)$$

where

V_{gn} = active gage voltage at the n^{th} stress level

V_{sn} = standard gage voltage at the n^{th} stress level

The voltage changes must then be put in a form so that the net strains may be calculated. The standard equation for determining strains from resistance changes of strains is:

$$\varepsilon = \frac{\Delta R_g}{(R_{go})\ (G.F.)}$$

where

ε = strain

G.F. = manufacturer's gage factor

R_{go} = original resistance of gage

ΔR_g = change in resistance of gage.

Since

$$R_{go} = R_{so} \frac{V_{go}}{V_{so}}$$

and

$$\Delta R_g = R_{so} \left(\frac{V_{gn}}{V_{sn}} - \frac{V_{go}}{V_{so}}\right),$$

then

$$\frac{\Delta R_g}{R_{go}} = \left(\frac{V_{so}}{V_{go}}\right)\left(\frac{V_{gn}}{V_{sn}} - \frac{V_{go}}{V_{so}}\right) = \left(\frac{V_{so}V_{gn}}{V_{go}V_{sn}} - 1\right) .$$

Therefore, the net strain in terms of voltages is

$$\varepsilon = \left(\frac{1}{G.F.}\right)\left(\frac{V_{so}V_{gn}}{V_{go}V_{sn}} - 1\right) .$$

The net strain was computed in this manner from the voltage measurements at zero stress level and each succeeding stress level. Assuming that the standard and active gages have the same original resistance and that 1.50000 volts is impressed across each, calculations yield about 3 microinch per inch strain for each 0.00001 voltage change. Therefore adequate circuit sensitivity is obtained using the above circuitry and a potentiometer which measures to 5 significant figures. In this study a scanning digital voltmeter (Dymec, Hewlett-Packard Instrument Company) was used to measure the voltages to 5 decimal places. The unit was set up to punch data tape which was computer processed to produce the net strains. The drift of this unit is about $\pm$ 0.00002 volt. Therefore, an uncertainty of about $\pm$ 6 microinch per inch strain exists in the processed data.

b. Slidewire Instrumentation

Three different types of slidewire transducers were designed and fabricated for measuring the deformations of rock and soil when subjected to a high hydrostatic pressure environment. The basic theory behind a slidewire transducer will be presented before describing the construction details of each of the three types. The general slidewire system is illustrated schematically in figure 15.

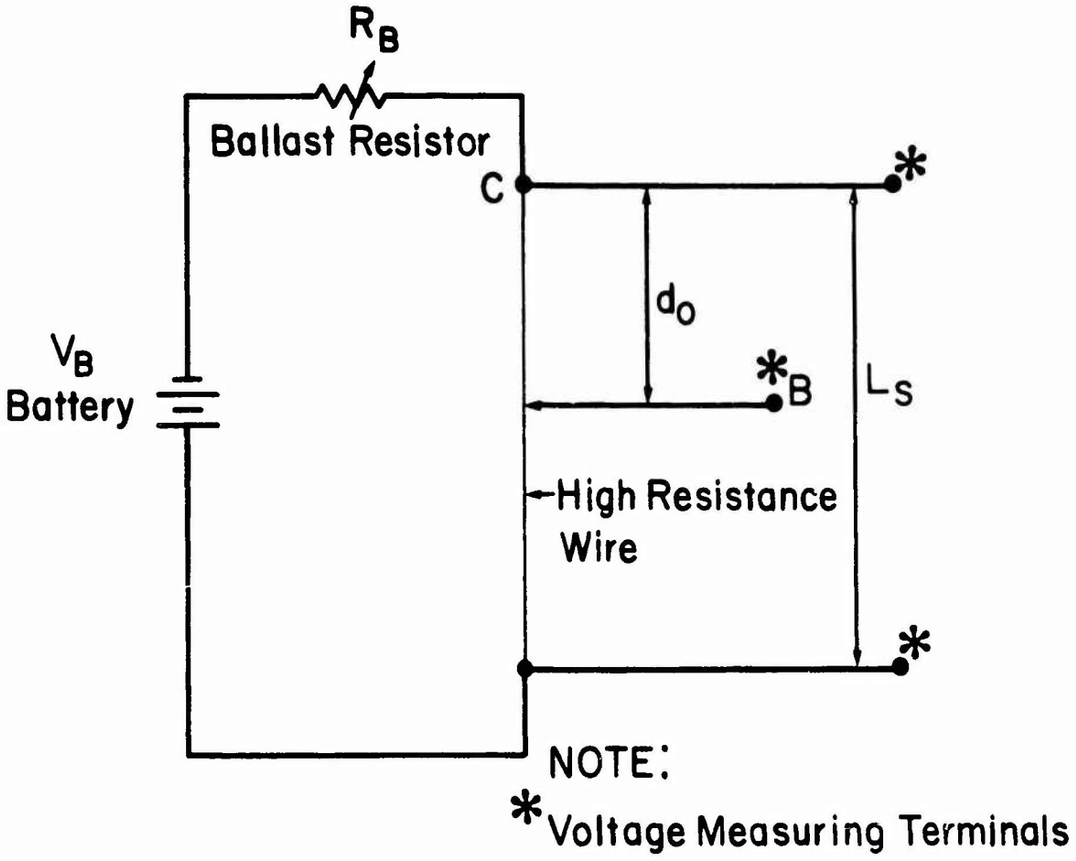

Figure 15. Slidewire Displacement Transducer Circuit

The slidewire transducers consist, essentially, of a fine, high-resistance wire along which three points are located for the purpose of obtaining voltages. Two of the points (A and C in figure 15) are fixed at a known distance apart. The voltage drop across AC provides what might be considered a standard voltage. The third point (B in figure 15) is variable, its position governed by the deformation of the material being studied. The voltage drop between this movable point and one of the fixed points, then, changes as the dimensions of the specimen change. The strain which the specimen experiences is found as follows:

With the arrangement shown in figure 15

$$V_B = V_b + V_{AC}$$

where

V_B = battery voltage
V_b = ballast resistor voltage
V_{AC} = voltage drop between points A and C.

The original position of the movable point, d_o, is given by

$$d_o = \left(\frac{V_{BC_o}}{V_{AC_o}} \right) L_s$$

where

V_{BC_o} = original voltage drop between points B and C
V_{AC_o} = original voltage drop between points A and C,
L_s = total slidewire length (distance between points A and C).

At the n^{th} stress level

$$\Delta n = \left(\frac{V_{BC_o}}{V_{AC_o}} - \frac{V_{BC_n}}{V_{AC_n}} \right) L_s$$

where

$(d_o - d_n) = \Delta n$ = displacement of the movable point due to deformation of the specimen.

The strain which the specimen experiences is given by

$$\varepsilon = \frac{\Delta L}{L_o}$$

where

ΔL = change in a given dimension

L_o = original magnitude of that dimension.

Therefore, in terms of the voltages, the strain experienced by the sample is

$$\varepsilon = \left(\frac{V_{BC_o}}{V_{AC_o}} - \frac{V_{BC_n}}{V_{AC_n}} \right) \frac{L_s}{L_o} .$$

The base sensitivity of the slidewire transducers is about the same as for the strain gages. This is shown in the following:

Assume

V_{BC_o} = 0.50000 volt

V_{AC_o} = 1.00000 volt

V_{BC_n} = 0.50002 volt

V_{AC_n} = V_{AC_o} = 1.00000 volt

L_s = 0.500 inch

L_o = 3.000 inches.

Using the above equation the strain sensitivity is about 4 microinch per inch.

All the slidewire transducers which were developed in this study are of the 5-terminal type. This arrangement is shown schematically in figure 16. Two of the leads are current leads for the high resistance wire, two leads are for measuring the voltage between the fixed points (represented by points A and C) and the remaining lead is connected to the movable point (represented by point B).

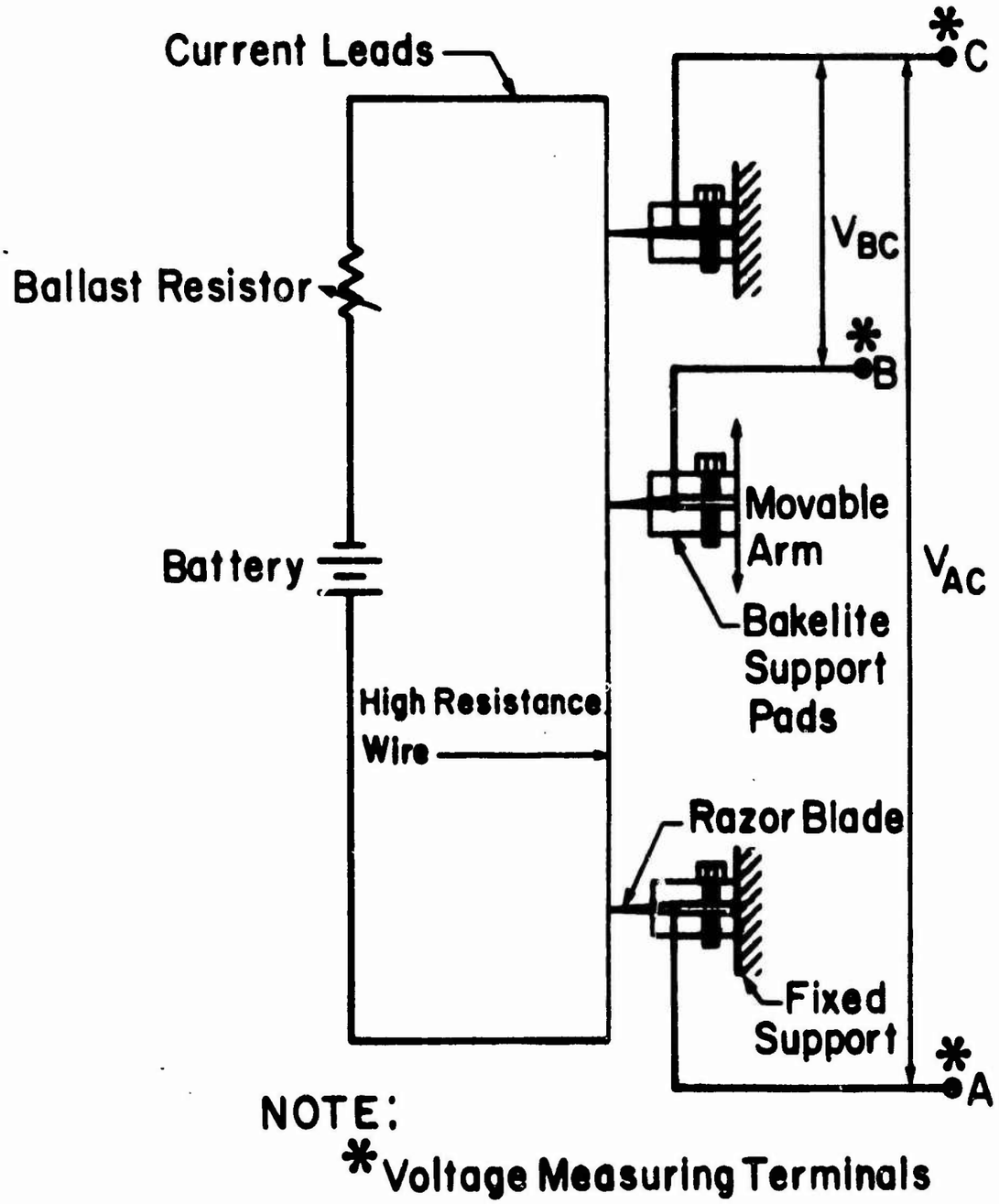

Figure 16. Schematic of Five Terminal Slidewire System

The slidewire fixture used most extensively in this study is shown in detail in figures 7 and 17. The wire is Chromel-R, 0.002 inch in diameter. It is fixed on one end to a screw and maintained in constant tension by means of a leaf spring. Contact is made with the wire by means of dulled razor blades. Two of the razor blades are fixed at a known distance apart. The other razor blade is affixed to a movable wiper arm which follows the deformation of the specimen. The entire device is insulated from the vessel by mounting the razor blades and screws into bakelite support pads.

In general, two axial slidewires were used simultaneously. They were placed 180 degrees apart to average the effects of any bending of the specimen which might occur. The diametrical slidewire is constructed with the support ring halved and pinned 180 degrees from the slidewire itself. Horizontal positioning and clamping screws are contained in the support ring at $\pm$ 90 degrees from the pinned connection (which is directly behind the specimen in figure 17). As changes in the diameter occur the pinned connection acts as a fulcrum and the movable razor blade moves a distance twice that of the change in diameter of the specimen.

The second type of slidewire which was developed is shown schematically in figure 18. Essentially it consists of a thin, high-resistance wire which is tensioned between the two springs, a tube and upper pad of Plexiglas, a razor blade which passes through the tube and contacts the wire, and two voltage leads which are spot-welded to the slidewire. The upper pad, which contacts the underside of the piston, is held in place by the upper spring. The lower spring is pretensioned so as to keep the slidewire tensioned when the upper pad moves downward, following the motion of the advancing piston. The two points, A and C, which are a fixed distance apart then, move relative to the fixed razor blade. Therefore the voltage between the point which contacts the razor blade (point B) and either point A or C changes as the piston advances. The axial slidewires are positioned 180 degrees apart

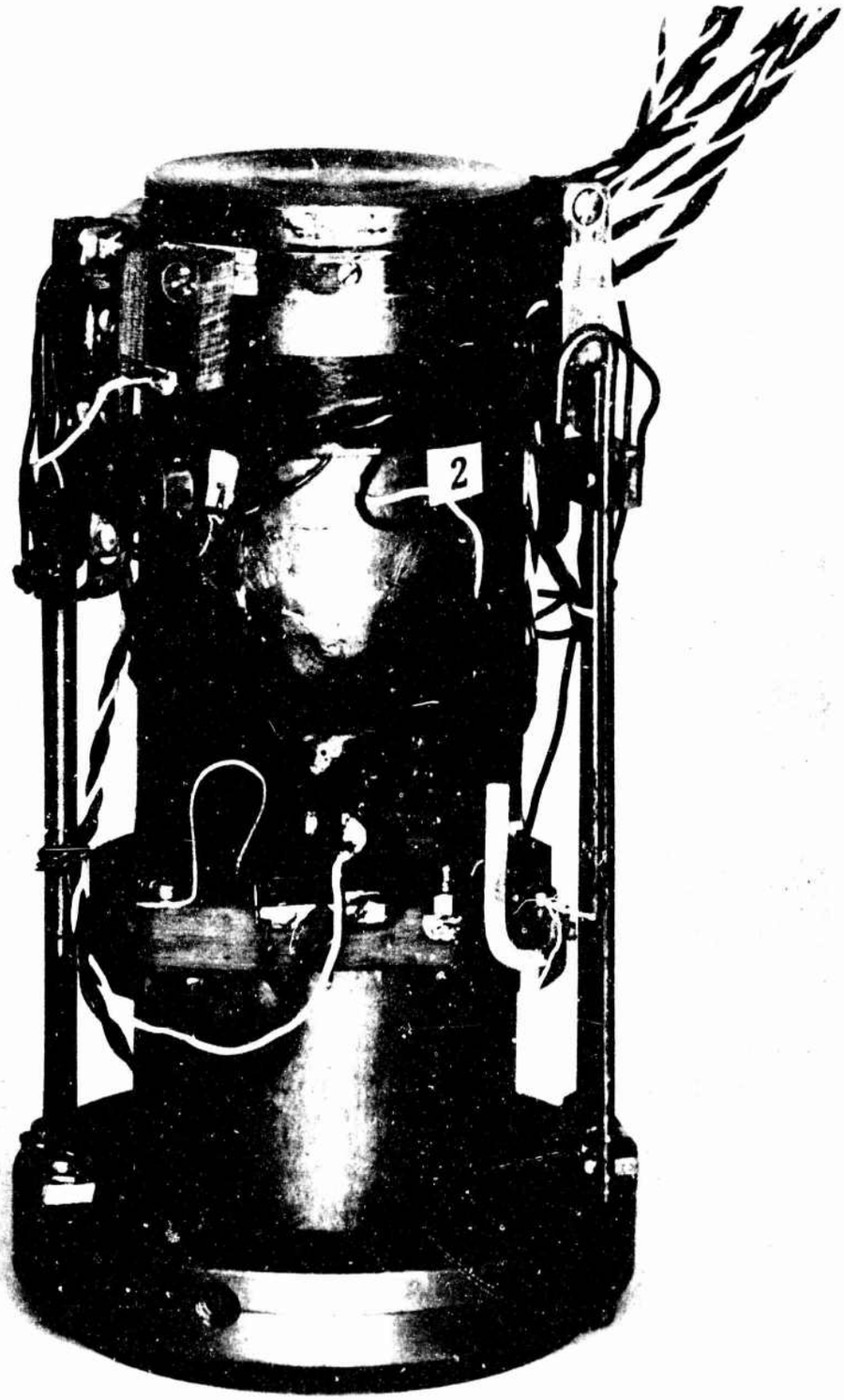

Figure 17. Detail of Slidewire Fixture for Confined Compression Tests

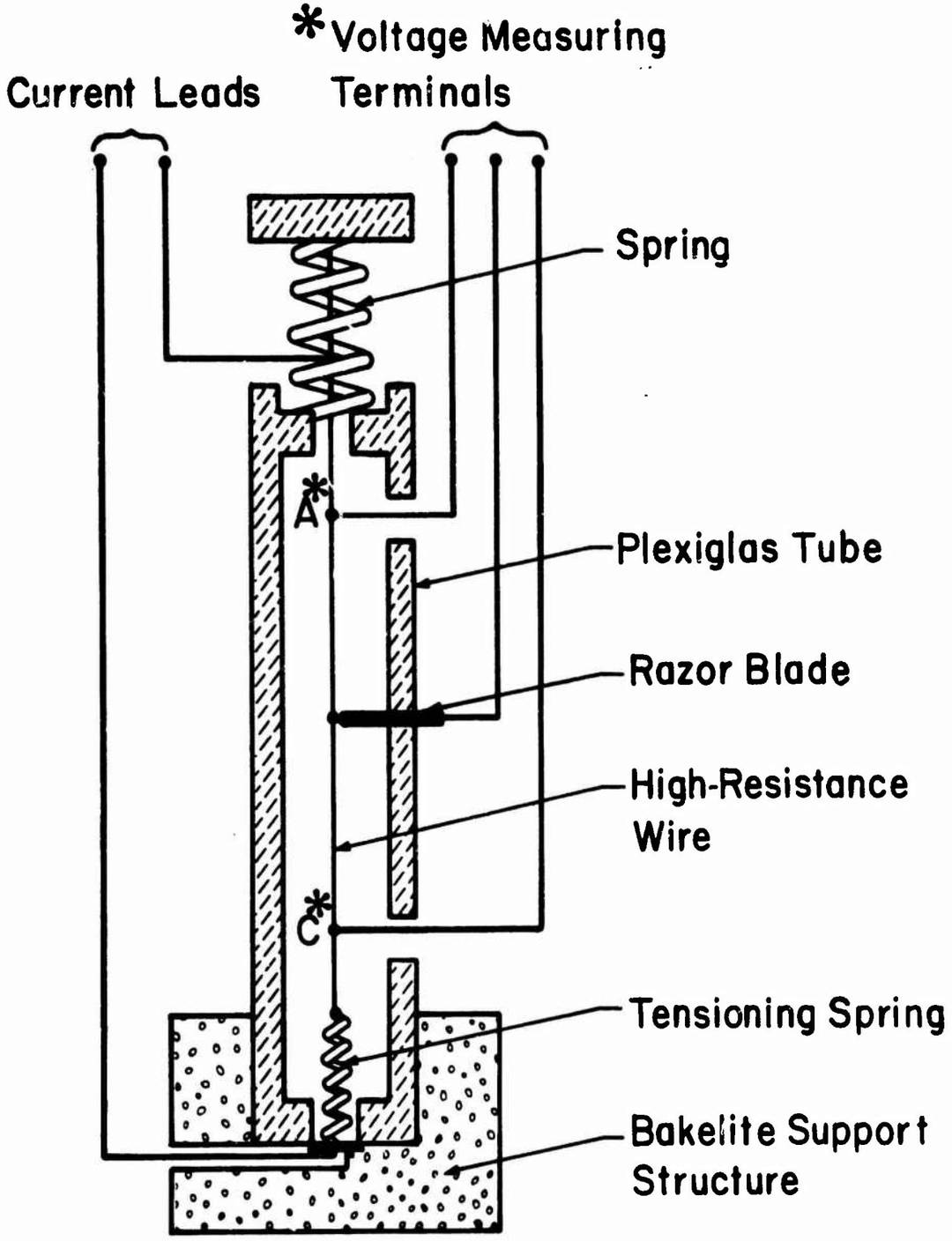

Figure 18. Schematic of Slidewire Transducer

and are held in place in bakelite support pads at the bottom of the confined compression apparatus. The horizontal slidewire, which measures changes in the diameter of the specimen, is held in place in the wall of the compression apparatus.

The third type of slidewire which was developed in this study is shown in figure 19. It consists of two co-axial Plexiglas tubes the smaller of which slides inside the other. The inner tube carries the slidewire, which is tensioned with the spring at the bottom, and brass screws which provide the fixed points for the standard voltage drop. The outer tube carries a third brass screw which provides the moving contact along the wire. The inner tube is held against the advancing piston by means of the spring which is connected to the inner tube and the outer tube. As the piston advances, then, the inner tube moves downward, carrying the slidewire past the fixed brass screw in the outer tube. Thus the change in voltage drop between the brass screw in the outer tube and either of the brass screws of the inner tube represents the displacement due to the motion of the piston. The upper spring, meanwhile, has been stretched so that when the load is removed and the piston returns upward, the inner tube will follow its motion. The entire device is held in place by fixing the outer tube to a bakelite support structure at the bottom of the confined compression jig. The support structure is shown in figure 19.

3. Specimen Preparation

a. Rock

The rock specimens were obtained by diamond coring. Subsequent to the coring the ends were sawed as flat as possible with a diamond saw and then were ground flat and parallel to within 0.0001 inch with a surface grinder. Prior to mounting strain gages the surface was slightly abraded with fine emery cloth and then cleaned thoroughly with acetone.

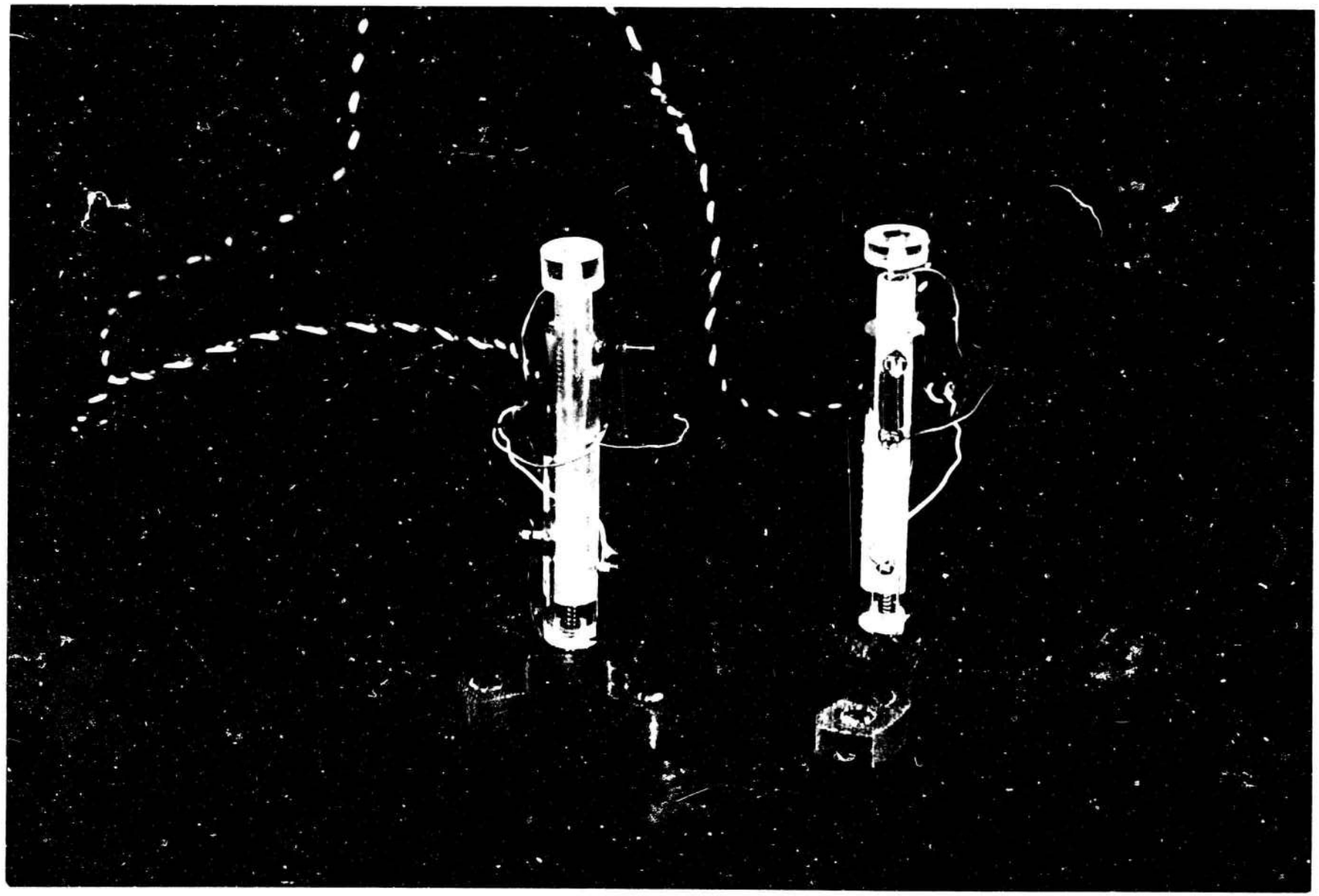

Figure 19. Slidewire Transducers

If encapsulation was required the samples were jacketed as follows: samples which were to be tested in a hydrostatic environment were jacketed with either a silicone rubber (General Electric RTV-102) or a latex rubber (Chicago Latex Products, Inc.). Samples to be tested in the confined compression jig required a slightly different technique so that a uniformly distributed end load could be applied to the specimen. A thin (0.002 inch) disc of stainless steel shim stock was placed over each end of the specimen. Next, spun copper caps were placed over the ends such as to extend down the sides of the sample for a short distance. The remainder of the sample was then coated with either of the two encapsulants mentioned above. Figure 20 shows two samples being prepared in this manner. The purpose of the steel shim was to prevent the possible intrusion of the copper into the end of the rock which might result in splitting of the sample.

b. Soil

The soil samples were encapsulated in either copper foil or the latex rubber mentioned above. Generally, it was possible to jacket the clay samples in the latex rubber since they were formed in a standard device used in soil mechanics laboratories wherein the sample would be encased in a thin rubber membrane. The sample could then be dipped in the liquid latex rubber for the final jacketing.

However, the thin rubber membrane would not support the sand samples. Therefore, copper was used for encapsulating the cohesionless soils. A container was fabricated from thin 0.005 inch copper foil and was filled with the cohesionless soil. The cover, of the same copper foil, was then soldered in place. Generally, the can was vibrated during the filling process so that the sand would be in a relatively close-packed condition.

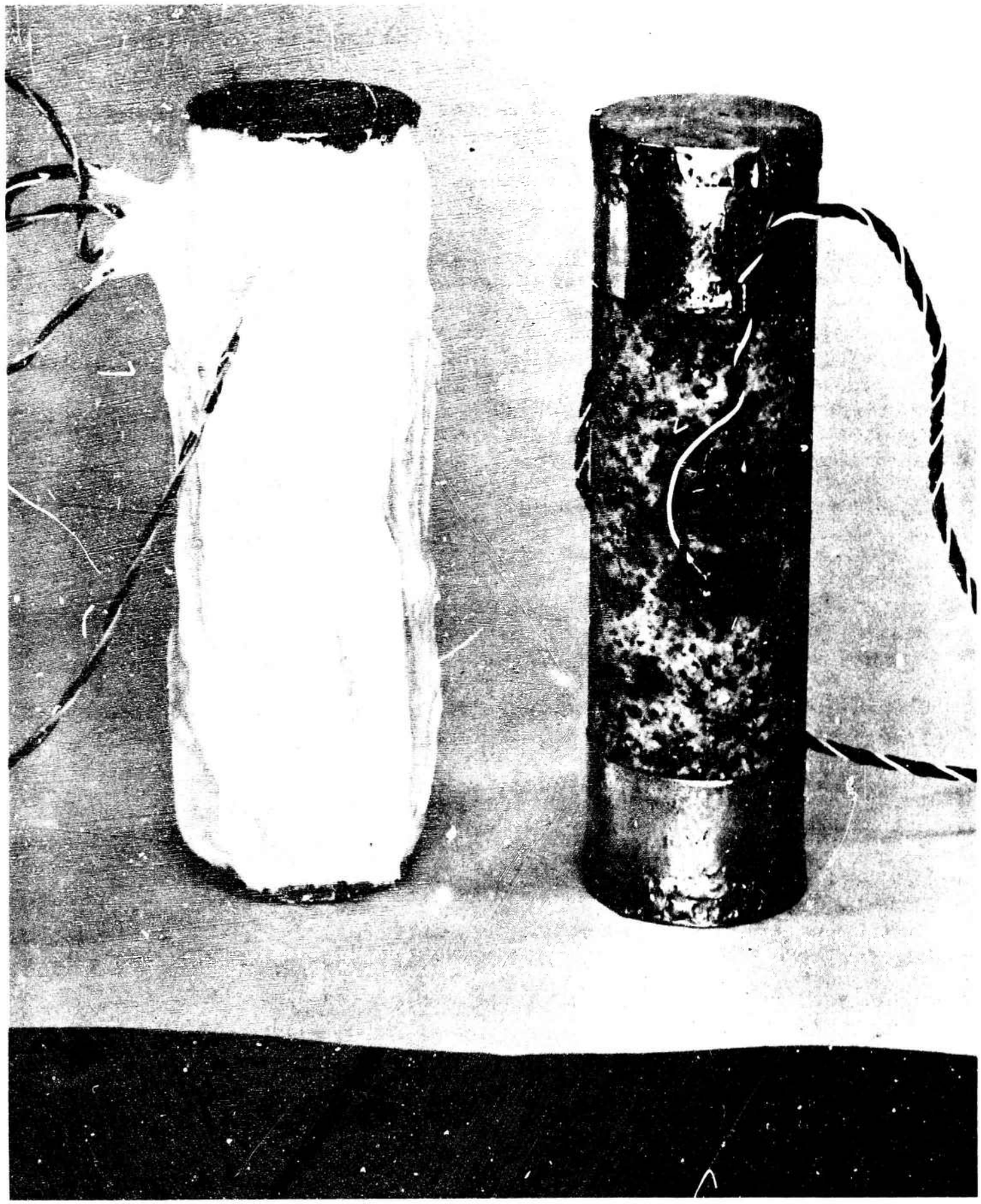

Figure 20. Encapsulating Procedure for Rock Samples

SECTION V

EXPERIMENTAL RESULTS

Tables I and II summarize the types of experiments performed during the course of this study. The first column gives the type of material used for the specimen. The dimensions of the specimens are given in the second column. The maximum pressure, either hydrostatic, as in the case of the compressibility tests, or confining, as in the case of the confined compression tests, is presented in the third column. The type of transducer for monitoring the deformation of the specimen, either strain gages or slidewires, or both, is given in the last column. The compression experiments,both uniaxial and confined, are presented in Table I. The bulk compressibility tests are presented in Table II.

The remainder of this chapter presents the experimental procedure and results for typical tests. This includes uniaxial compression of granite specimens to study the effect of frictional constraint imposed on the ends of the specimen, confined compression tests on steel, diorite, kaolinite clay and Ottawa sand; compressibility tests on diorite, granite, kaolinite clay and Ottawa sand, and a torsional test on granite.

Typical stress-strain curves and compressibility curves for each of the experiments are presented to show the effect of pressure on the stress tensors.

1. Uniaxial and Confined Compression Tests

a. Uniaxial Compression Test on Granite

Uniaxial compression tests were conducted on three samples of the biotite granite to observe the effect of frictional constraint at the ends of the specimen. The samples were circular cylinders with a diameter of 1 inch. The length to diameter ratios were 1, 2 and 5. Two diametrically opposed strain gages were placed

Table 1

SUMMARY OF CONFINED COMPRESSION EXPERIMENTS

Material	Specimen Dimensions (in.)	Maximum Vessel Pressure (psi)	Transducers*	
			S.G.	S.W.
Steel	1 1/2 D x 3	0	X	
Steel	1 1/2 D x 3	0	X	X
Steel	1 1/2 D x 3	0	X	X
Steel	1 1/2 D x 3	40,000	X	X
Steel	1 1/2 D x 3	56,000	X	X
Granite	1 D x 1	0	X	
Granite	1 D x 3	0	X	
Granite	1 D x 5	0	X	
Granite	1 1/4 D x 3	0	X	
Granite	1 1/4 D x 5 3/4	0	X	
Granite	1 1/2 D x 3	0	X	
Granite	1 1/2 D x 3	40,000	X	X
Granite	1 1/2 D x 3	40,000	X	X
Granite	1 1/2 D x 4	50,000	X	
Diorite	1 1/2 D x 4	50,000	X	
Limestone	1 1/2 D x 3	0	X	
Limestone	1 1/2 D x 3	0	X	
Clay	1 1/4 D x 2 1/2	7,000		X
Ottawa Sand (Dry)	1 1/2 D x 4	25,000		X

* Denotes strain gages and/or slidewires.

Table II

SUMMARY OF COMPRESSIBILITY EXPERIMENTS

A) Compressibility Experiments

Material	Specimen Dimensions (in.)	Maximum Vessel Pressure (psi)	Transducers*	
			S.G.	S.W.
Steel	1 1/2 D x 4	55,000	X	
Steel	1 1/2 D x 4	55,000	X	
Steel	3 D x 3	65,000		X
Steel	3 D x 3	69,500		X
Granite	3 D x 6	55,000	X	
Diorite	3 D x 6	55,000	X	
Diorite	3 D x 3	55,000		X
Diorite	3 D x 3	106,000		X
Limestone	1 1/2 D x 4	55,000	X	
Limestone	1 1/2 D x 4	55,000	X	
Ottawa Sand (Dry)	3 D x 3	10,000		X
Ottawa Sand (Dry)	3 D x 3	16,000		X
Ottawa Sand (Dry)	3 D x 3	106,000		X
Clay	3 D x 3	15,000		X
Clay	3 D x 3	32,000		X

* Denotes strain gages and/or slidewires.

on each sample at midheight. The load versus axial strain curves for the samples are presented in figures 21, 22 and 23.

The large difference between the axial strains at the same load levels indicates that bending occurred even though precautions were taken to eliminate it; specifically, (1) by grinding the sample ends flat and parallel and (2) by compressing the samples between spherically-seated platens. The modulus of elasticity, E , was determined from the slope of the average load versus axial strain curve. Notice that the elastic modulus was 8.0×10^6 psi for the two samples of length to diameter ratio equal 3 and 5 but significantly higher (9.4×10^6 psi) for the sample of L/D equal to one. This indicates that the frictional constraint imposed on the ends of the sample has a significant effect on the stress state in the specimen and that care must be taken to either (1) remove the frictional constraint or (2) take measurements at points sufficiently far from the ends so that the stress field is uniform and predictable.

b. Confined Compression Test on Steel

Uniaxial and confined compression tests were performed on steel (C-1018) specimens so that the slidewire and strain gage techniques could be tested on a material of known characteristics. The confined compression apparatus was used for these tests. (The apparatus is described in Section IV). A stress-strain curve obtained during a uniaxial compression test on steel is presented in figure 24. The axial strain given in figure 24 is the average output of four strain gages placed 90 degrees around the circumference of the sample. The average value of Poisson's ratio was obtained from the output of two circumferential strain gages placed 180 degrees apart around the circumference of the sample. The values of the modulus of elasticity and Poisson's ratio agree with the usual values found in the literature.

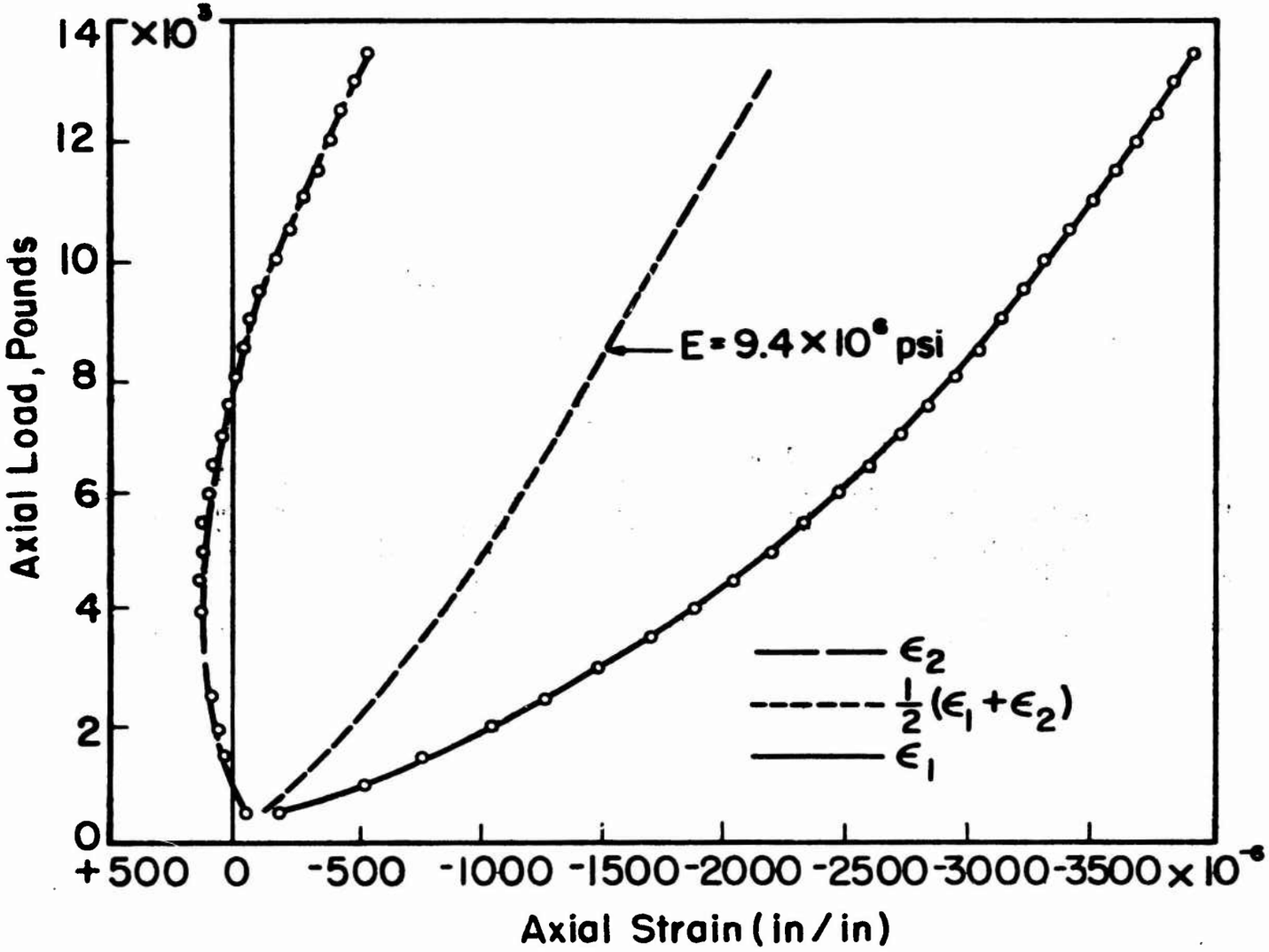

Figure 21. Uniaxial Compression of Granite - L/D = 1

Figure 23. Uniaxial Compression of Granite - L/D = 5

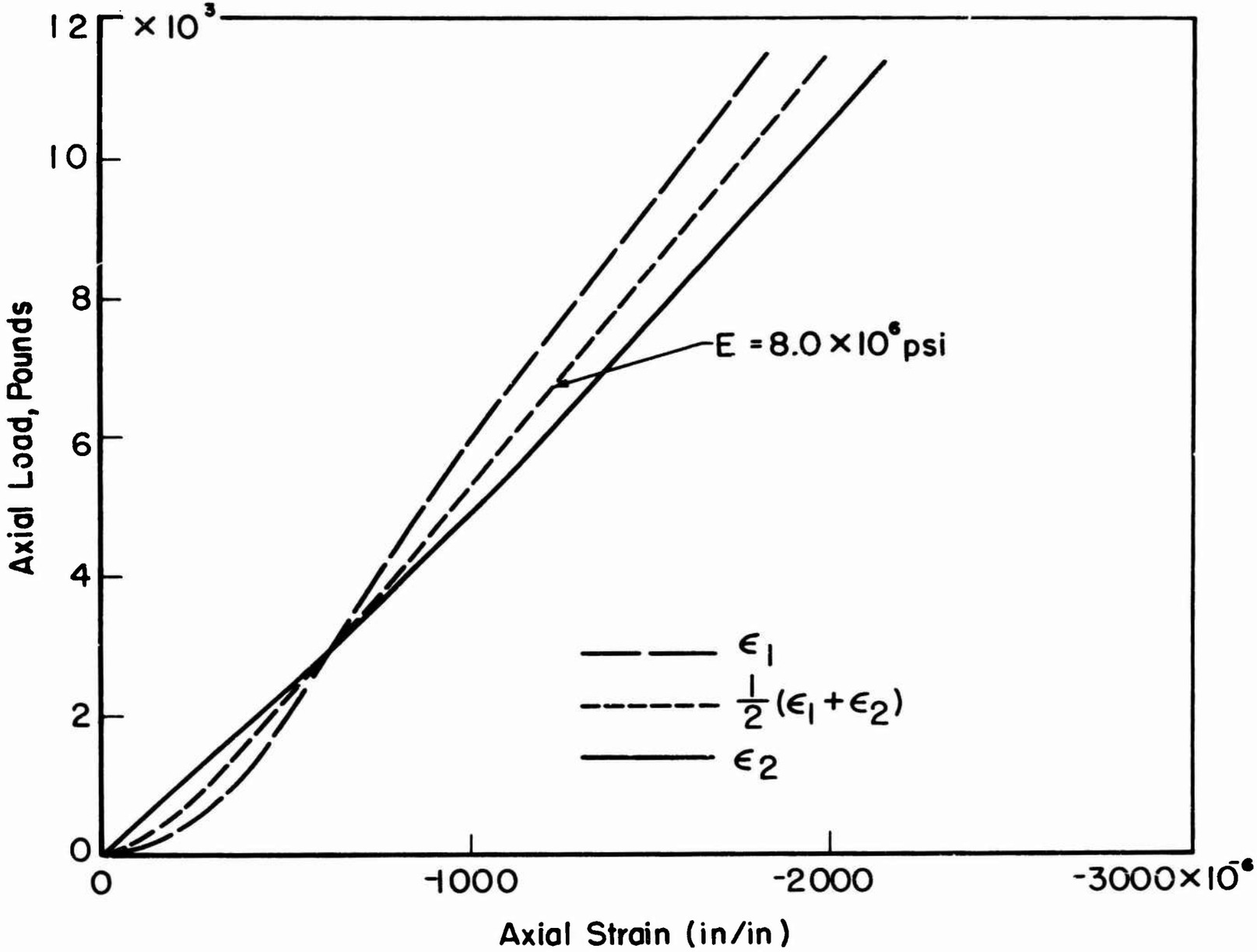

Figure 22. Uniaxial Compression of Granite - L/D = 3

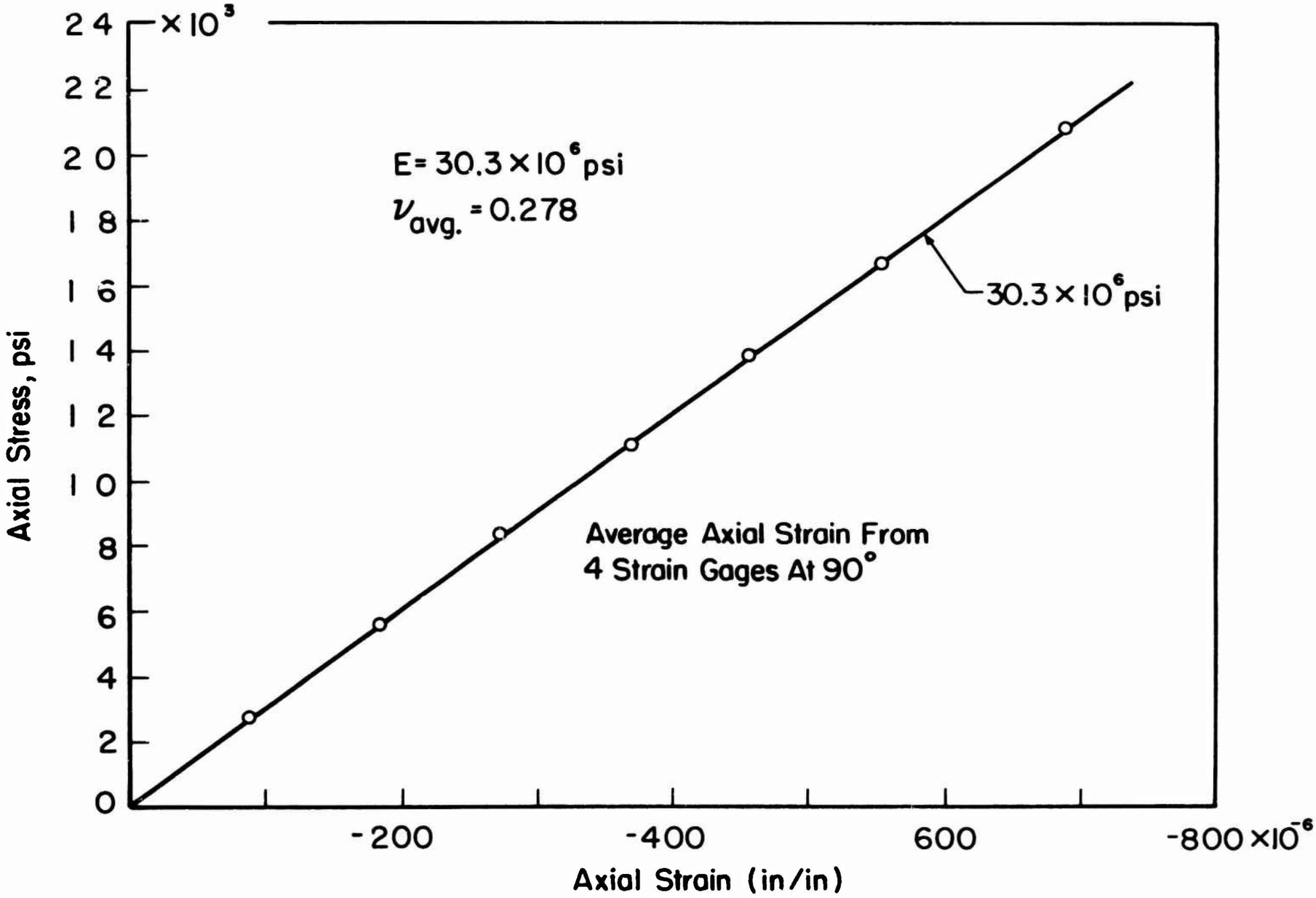

Figure 24. Uniaxial Compression of Steel

Both axial and diametrical slidewire displacement transducers were also used during this experiment. While the diametrical slidewire produced measured strains which were in good agreement with the lateral strain gages, the axial slidewires did not agree with the axial strain gages. Presumably this was due to insufficient pre-tensioning of the slidewire so that the slidewire tended to sag and lose contact with the movable razor blade.

c. Confined Compression Test on Diorite

Using the aforementioned compression fixture and the techniques described in an earlier section, a confined compression experiment on diorite was performed. The results of the experiment are summarized in figure 25. This figure shows the stress-strain curve for the material in a pressure environment of 40,000 psi. The plotted axial strains are the averages taken from gages 180 degrees apart to average the effects of bending. The figure shows that a modulus of elasticity of 10×10^6 psi was obtained from both sets of gages at the 40,000 psi pressure plateau. Values of modulus of elasticity and Poisson's ratio obtained at the other pressure levels are presented in figure 25.

d. Confined Compression Tests on Ottawa Sand

Confined compression tests were conducted on a cylindrical sample of dry Ottawa sand. The specimen had an original diameter and length of 1.5 inches and 4 inches respectively, and was encapsulated in copper foil. Close packing was obtained by vibrating the can during the emplacement of the sand. The sample was placed in the confined compression apparatus and instrumented with two axial slidewires placed 180 degrees apart and one horizontal slidewire.

Data was obtained as follows: The specimen was subjected to a hydrostatic pressure of approximately 5000 psi. The axial stress on the sample was then increased by increasing the pressure above the movable piston in the confined compression fixture.

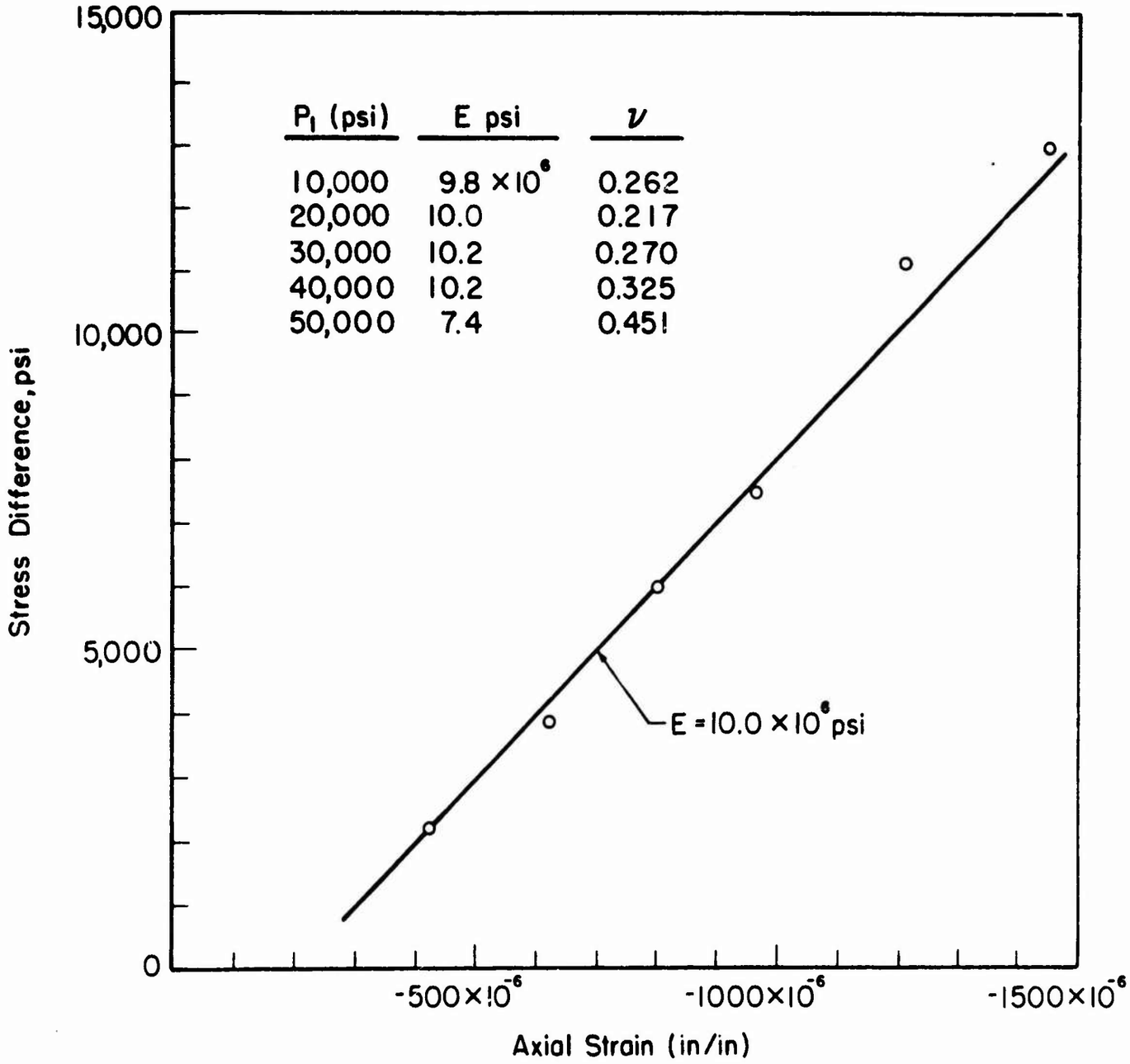

Figure 25. Results of Confined Compression Tests on Diorite

Data points were obtained by simultaneously recording the pressure above the movable piston and the displacements of the axial slidewires. Three or four points of pressure and displacement were obtained at a given level of confining pressure. This constituted the data for constructing a stress-strain curve. Additional stress-strain curves were obtained under confining pressures of 6700, 8000, 9000, 10,000, 15,000, 20,000 and 25,000 psi. The test was terminated before reaching a confining pressure of 30,000 psi because the jacketing leaked. Representative stress-strain curves for the confined compression tests on Ottawa sand are shown in figure 26. The maximum possible error is represented by the vertical and horizontal bars. The slopes represent the apparent values of Young's modulus.

e. Confined Compression Test on Kaolinite Clay

A cylindrical sample of nearly saturated (95 percent) kaolinite clay was subjected to confined compression tests up to a confining pressure of 7000 psi. The sample was initially subjected to a 1000 psi hydrostatic state of stress before the axial stress increased. No meaningful data were obtained from this test due to the fact that it was impossible to develop any stress difference in the sample. That is, it was apparently impossible to increase the axial stress above that of the lateral confining pressure. This was thought to be due to the possibility that, under pressure, the sample became fully saturated, which resulted in a hydrostatic state of stress in the sample. The sample was subjected to increasing levels of confining pressure up to 7000 psi but it was still unable to support any detectable stress difference. The test was, therefore, terminated at 7000 psi.

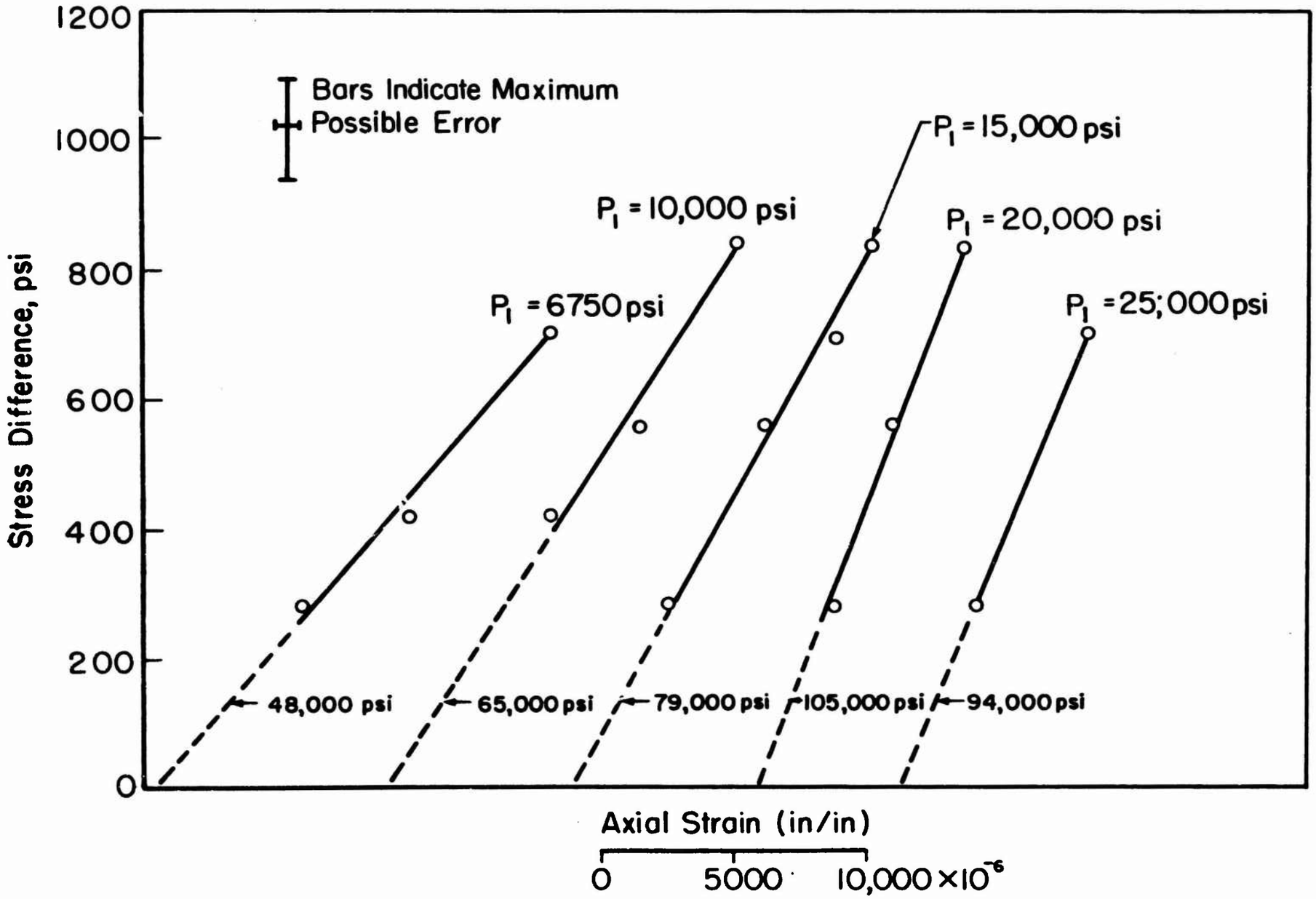

Figure 26. Results of Confined Compression Tests on Ottawa Sand (dry)

2. Bulk Compressibility Tests

a. Compressibility Test on Diorite

The bulk compressibility of an unjacketed sample of quartz diorite was measured to 55,000 psi in the compressibility fixture described earlier (Section IV). One of the two chambers in the fixture was filled with a solid steel cylinder and oil. The other chamber contained the rock sample, a steel sheath, and an amount of oil equal to that in the chamber containing the steel specimen. Displacement of the pistons during the pressure increments was measured with the potentiometer slidewire system described elsewhere (Section IV).

The curves of pressure versus piston displacement are presented in figure 27. The bulk compressibility of the rock sample is found in the following manner.

For the chamber which contains the steel and oil, the displacement of the piston due to the compressibility of the oil is found by subtracting the displacement due to the compressibility of the steel from the total displacement.

The bulk compressibility of steel is $4.55 \times 10^{-8} \text{psi}^{-1}$. Therefore at 55,000 psi the volumetric strain of steel is

$$\left(\frac{\Delta V}{V}\right)_s = (4.55 \times 10^{-8}\text{psi}^{-1}) \quad (55 \times 10^{3}\text{psi}) = 2.5 \times 10^{3}$$

The height of the chamber containing the steel and oil is 3.58 inches The displacement, σ, corresponding to a volumetric strain of 2.5×10^{-3} is

$$\sigma = (3.58) \quad (2.5 \times 10^{-3}) = 8.95 \times 10^{-3}$$

$$= 8950 \times 10^{-6} \text{ inch.}$$

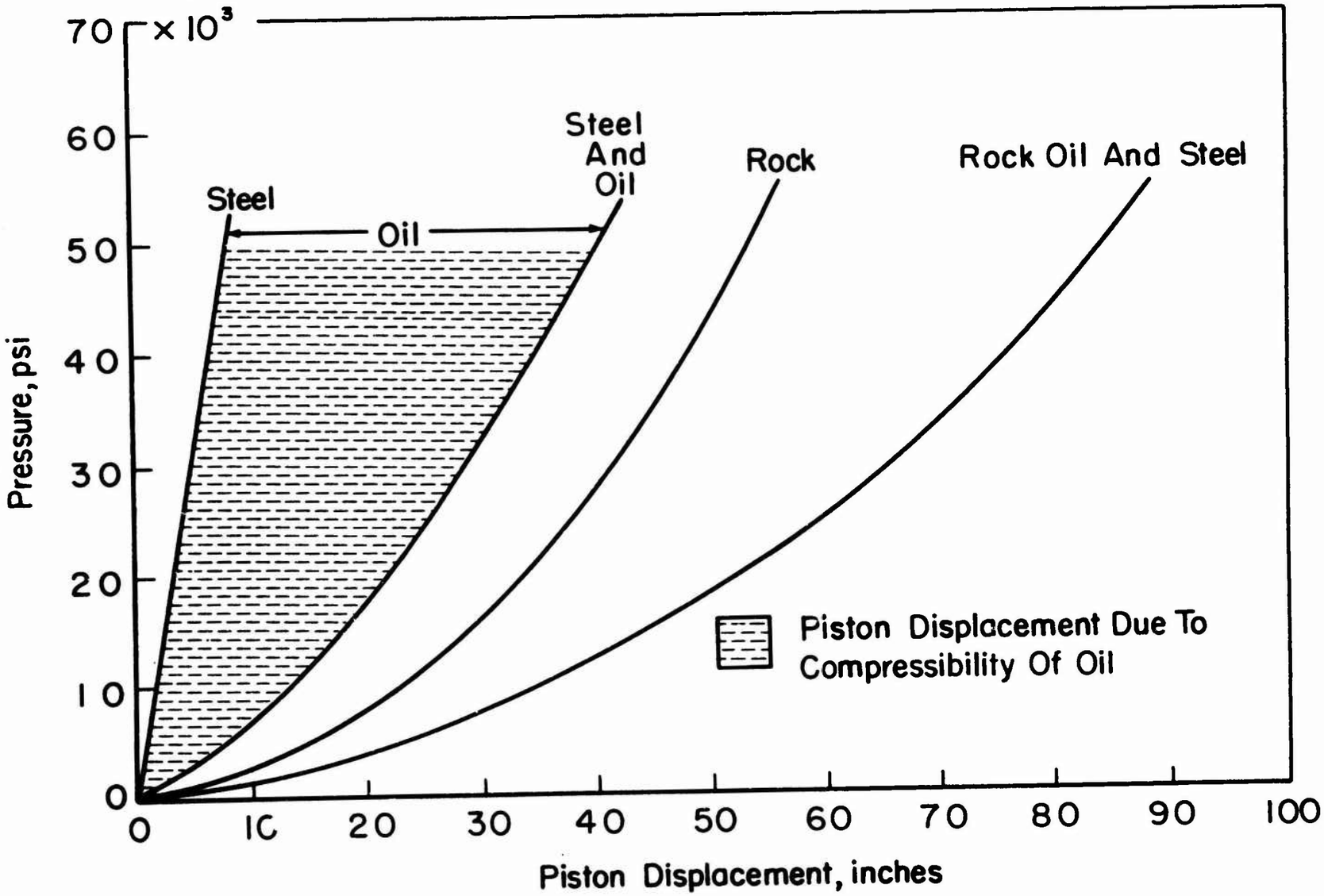

Figure 27. Results of Bulk Compressibility Test on Diorite

On figure 27 the displacement due to the compressibility of the steel at each pressure level is shown by the straight line passing through zero and the point (55,000 psi, 8950 x 10^{-6} inch). The displacement, at each pressure level, due to the compressibility of the oil, then, is given by the difference between the total displacement and that due to the steel.

The displacement due to the compressibility of the rock is then found by subtracting the displacements due to the oil and steel from the total displacement of the chamber containing the rock specimen. The displacement due to the compressibility of the steel sheath at 55,000 psi is

$$(8950 \times 10^{-6} \text{ inch}) \left(\frac{\text{Volume Steel Sheath}}{\text{Volume Steel Cylinder}} \right) = (8950 \times 10^{-6}) \left(\frac{5.42}{31.66} \right)$$

$$= 1530 \times 10^{-6} \text{ inch.}$$

which amounts to somewhat less than 2 percent of the total displacement and for all practical purposes can be ignored.

The pressure versus displacement curve for the rock is shown in the figure and is obtained by subtracting the displacement due to the compressibility of the oil from the curve of pressure versus total displacement.

The bulk compressibility is found by taking the inverse of the slope of the pressure versus displacement curve for the rock and dividing it by the total length of the chamber. Above 35,000 psi the curve is linear and the inverse of the slope is 5.47 x 10^{-7} inch per psi. Therefore, the bulk compressibility of the rock is

$$\frac{5.47 \times 10^{-7} \text{ in./psi}}{3.58 \text{ in.}} = 1.53 \times 10^{-7} \text{ psi}^{-1}$$

This value is comparable to those reported for similar rock types.[6]

The nonlinearity of the pressure versus displacement curve may be due to either or both of two causes: (1) the oil is entering the rock and (2) internal cracks are closing during the initial pressure increments (as described in Section II).

b. Compressibility Test on Ottawa Sand

The bulk compressibility of dry 20-40 Ottawa sand was measured to a pressure of 16,000 psi in the compressibility apparatus. The sample was jacketed in 0.005 inch copper foil. As can be seen from the pressure versus displacement curve, figure 28, the jacket leaked at about 10,000 psi.

As with the other compressibility tests, the piston displacements due to the compressibility of the oil must be subtracted from the total displacements to find the compressibility of the sand. The volume of the sand sample was 27.0 inches, therefore, the oil volume was 6.8 inches. When this correction is applied, the pressures versus piston displacement curve for the sand appears as shown in the figure. The curve is essentially linear above a pressure of 3000 psi. The bulk compressibility of the sand is found by dividing the inverse of the slope of the pressure versus piston displacement curve by the total height of the chamber.

$$\beta = \frac{63.3 \times 10^{-7} \text{ in./psi}}{3.58 \text{ in.}} = 17.7 \times 10^{-7} \text{ psi}^{-1}$$

c. Compressibility Test on Kaolinite Clay

The bulk compressibility of a jacketed sample of kaolinite clay was found to a pressure of 32,000 psi as in the other experiments. The sample was prepared by mixing water and pure kaolinite to a water content of about 40 percent. The clay was then placed in a can made from 0.005 inch copper foil. The sample was compacted in the copper can so that the saturation was about 95 percent. The total volume of clay was 24.4 cubic inches. The remaining volume of the chamber (33.8 - 24.4 = 9.4 cu. in.) was filled with oil.

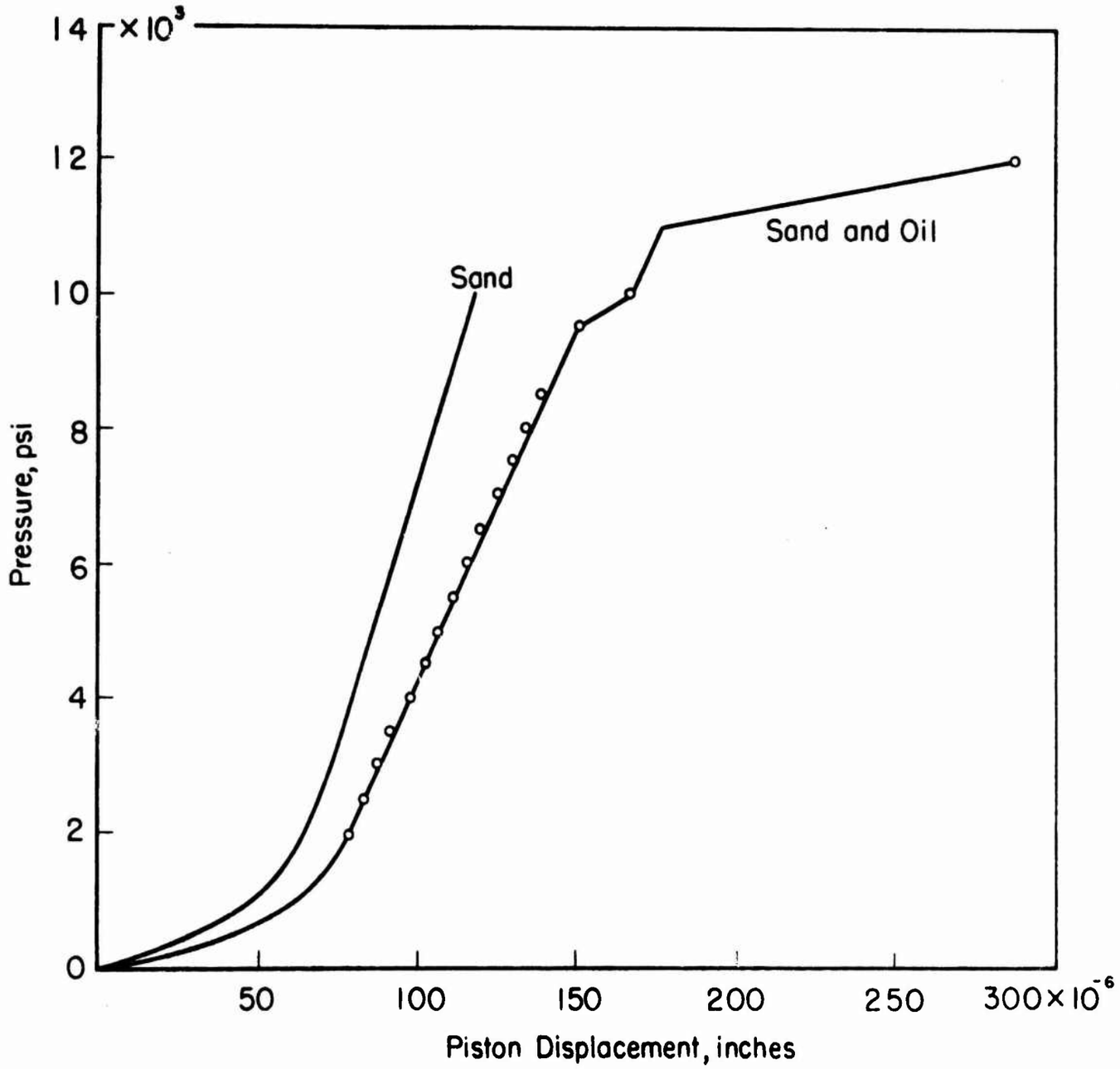

Figure 28. Results of Bulk Compressibility Tests on Ottawa Sand (dry)

The pressure versus piston displacement curve is shown in figure 29. The displacement due to the compressibility of the clay was found by subtracting the displacement due to the compressibility of the oil from the total displacements. (This was done in the same manner as in the compressibility test on the quartz diorite.)

As seen from figure 29, the pressure versus displacement curve for the clay is essentially linear above 10,000 psi. The bulk compressibility of the clay above 10,000 psi then is

$$\frac{31.6 \times 10^{-7} \text{ in./psi}}{3.58 \text{ in.}} = 8.8 \times 10^{-7} \text{ psi}^{-1}$$

This low compressibility (about five times that of solid quartz) is perhaps due to the fact that the clay is fully saturated above a pressure of 10,000 psi (which is reasonable since the original saturation was about 95 percent) and the volumetric strain is due to the compressibility of the entrapped water and clay particles.

d. Compressibility Test on Granite, Elevated Temperature

One bulk compressibility test was conducted at 150 degrees F to determine the suitability of the facility for measuring the mechanical properties of rock at elevated temperatures. An unjacketed cylinder of granite was used for the sample. The specimen had a diameter and length of 2 and 4 inches, respectively. The deformations were monitored by means of strain gages. The results of the test are shown in figure 30. As can be seen from figure 30, the plot of pressure versus volumetric strain is linear above about 20,000 psi. The slope of the linear portion represents a bulk compressibility of 1.375×10^{-7} psi $^{-1}$ which is comparable to values obtained by Brace for a granite.[6]

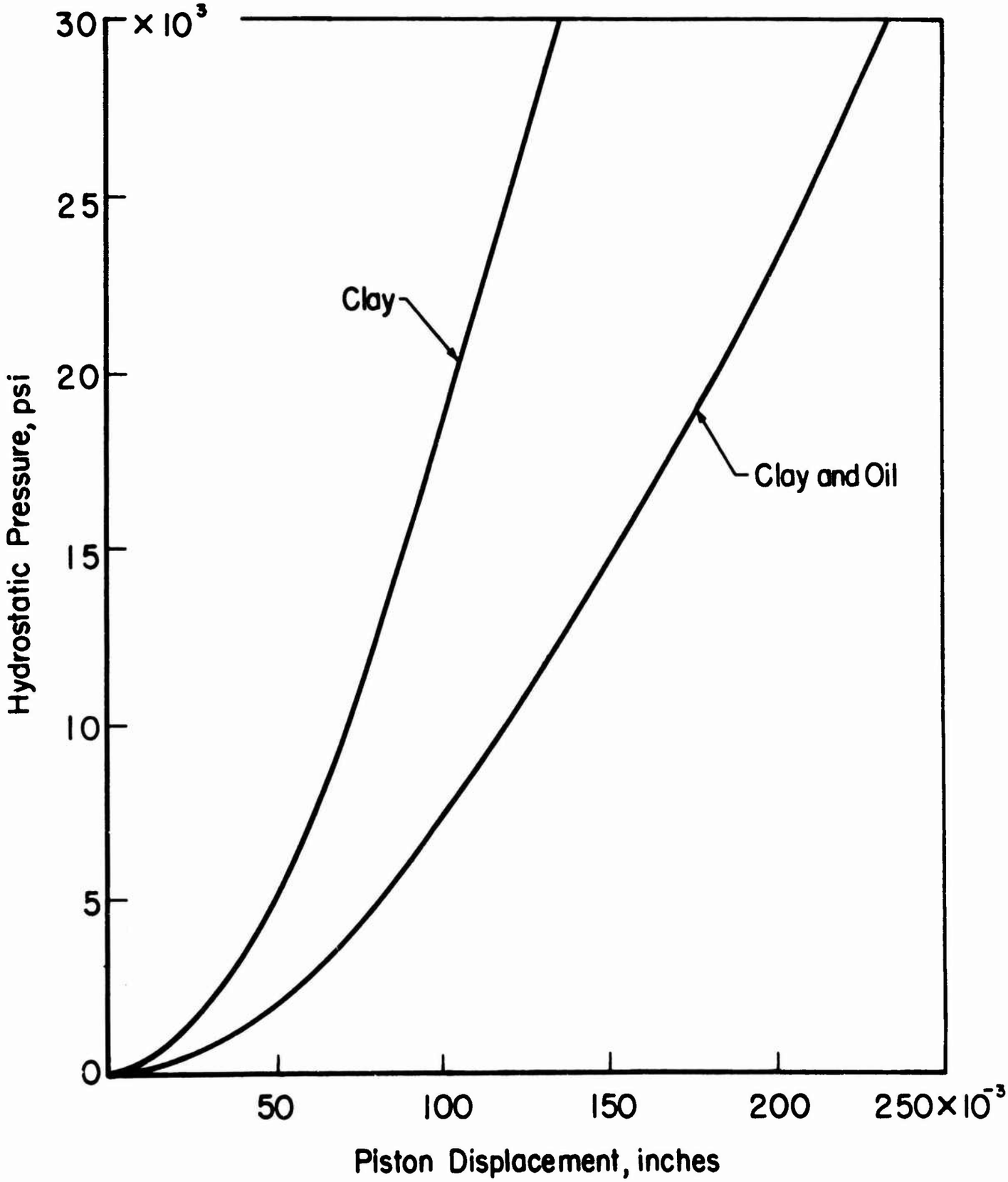

Figure 29. Results of Bulk Compressibility Test on Kaolinite Clay

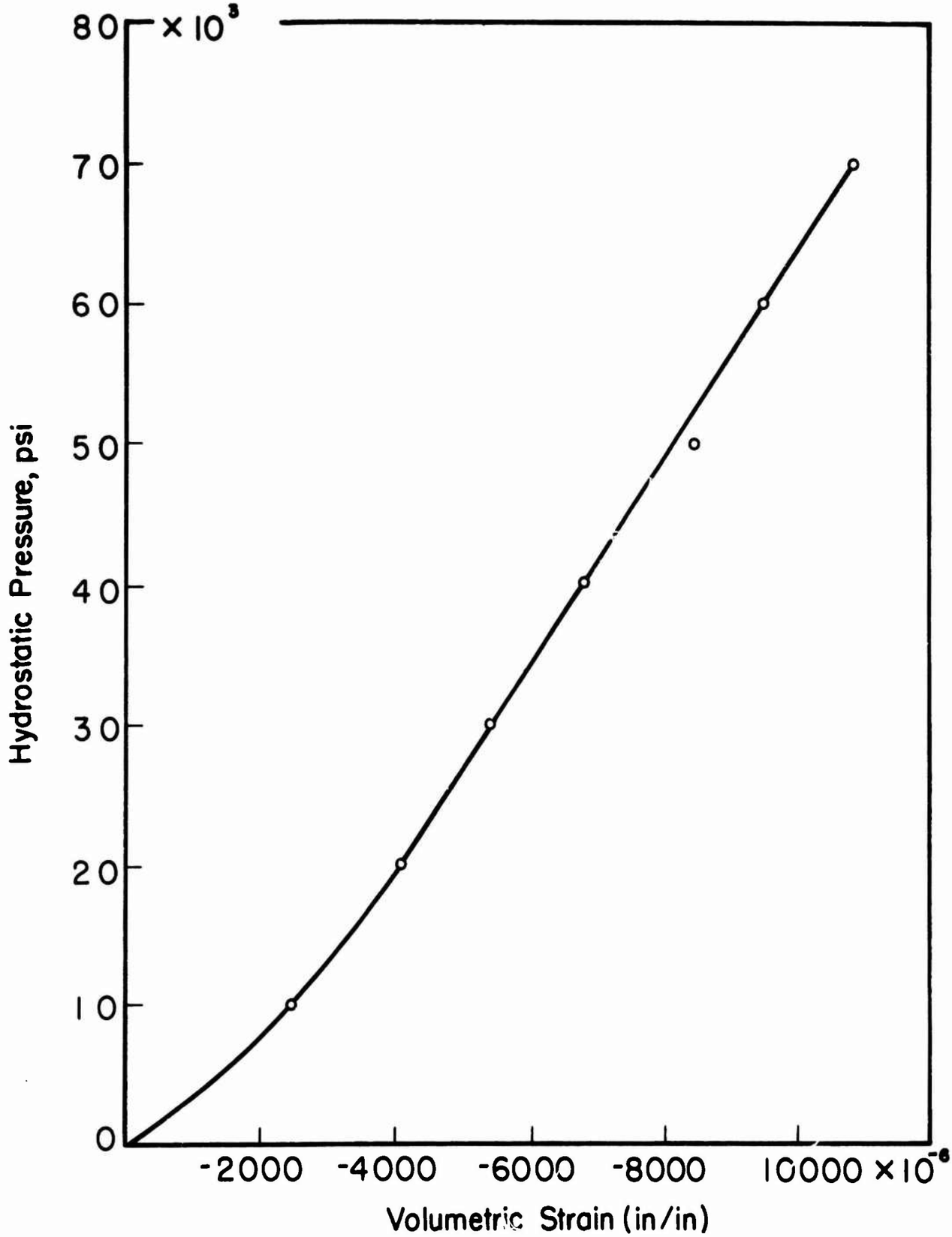

Figure 30. Bulk Compressibility of Granite at 150° F

3. Torsion Test on Granite

An ambient pressure torsion test was conducted on a hollow cylinder of biotite granite. Two pairs of orthogonal strain gages were placed on the specimen. Each gage was inclined at 45 degrees to the cylindrical axes so as to monitor the principal strains. When placed in this configuration, two of the strain gages experience a compressional strain and two experience a tensional strain. Advantage was taken of this fact by incorporating the four gages into the four arms of a Wheatstone bridge as shown in figure 31. The strains measured with the strain indicator are the sum of the absolute values of the four individual strains. The average value of the principal strains, $\bar{\varepsilon}$, was found by dividing this total strain by four.

The torsional cell was calibrated by the application of known torques furnished by calibrated weights. Torque was transmitted to the rock specimen by means of interlocking "turrets". The load cell output and the strains in the rock specimen were monitored at each load level. The output of the load cell was converted to torque which was subsequently plotted against the average individual strains experienced by the rock sample. The torque versus average strain curve is shown in figure 32.

The shearing modulus, G, is given by

$$G = \frac{\tau}{\gamma}$$

τ = shear stress

γ = shear strain

For a hollow cylinder under a torque, T , the maximum stress is given by

$$\tau = \frac{2R_1 T}{\pi(R_1^4 - R_o^4)}$$

where

R_1 = outer radius

R_o = inner radius.

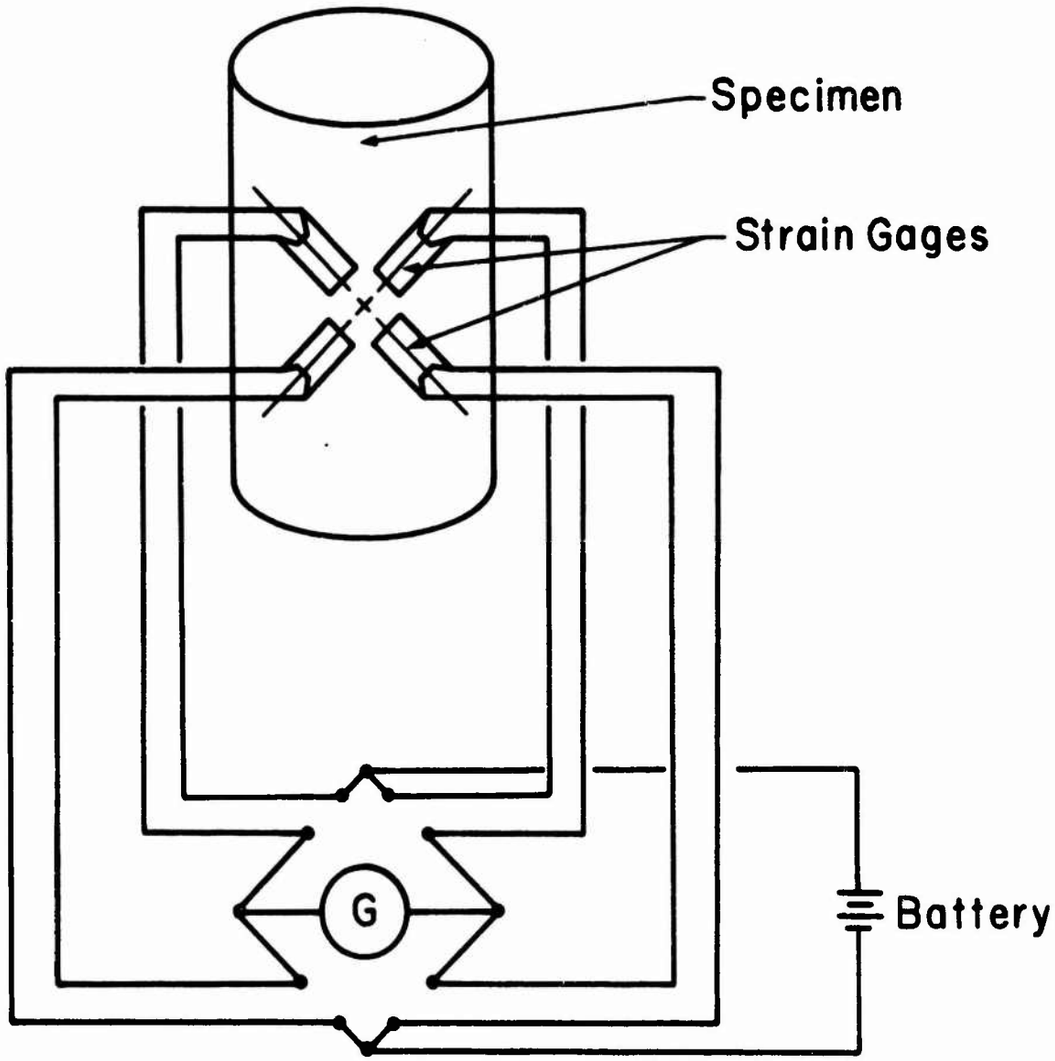

Figure 31. Strain Gage - Wheatstone Bridge Circuit for Torsion Experiments

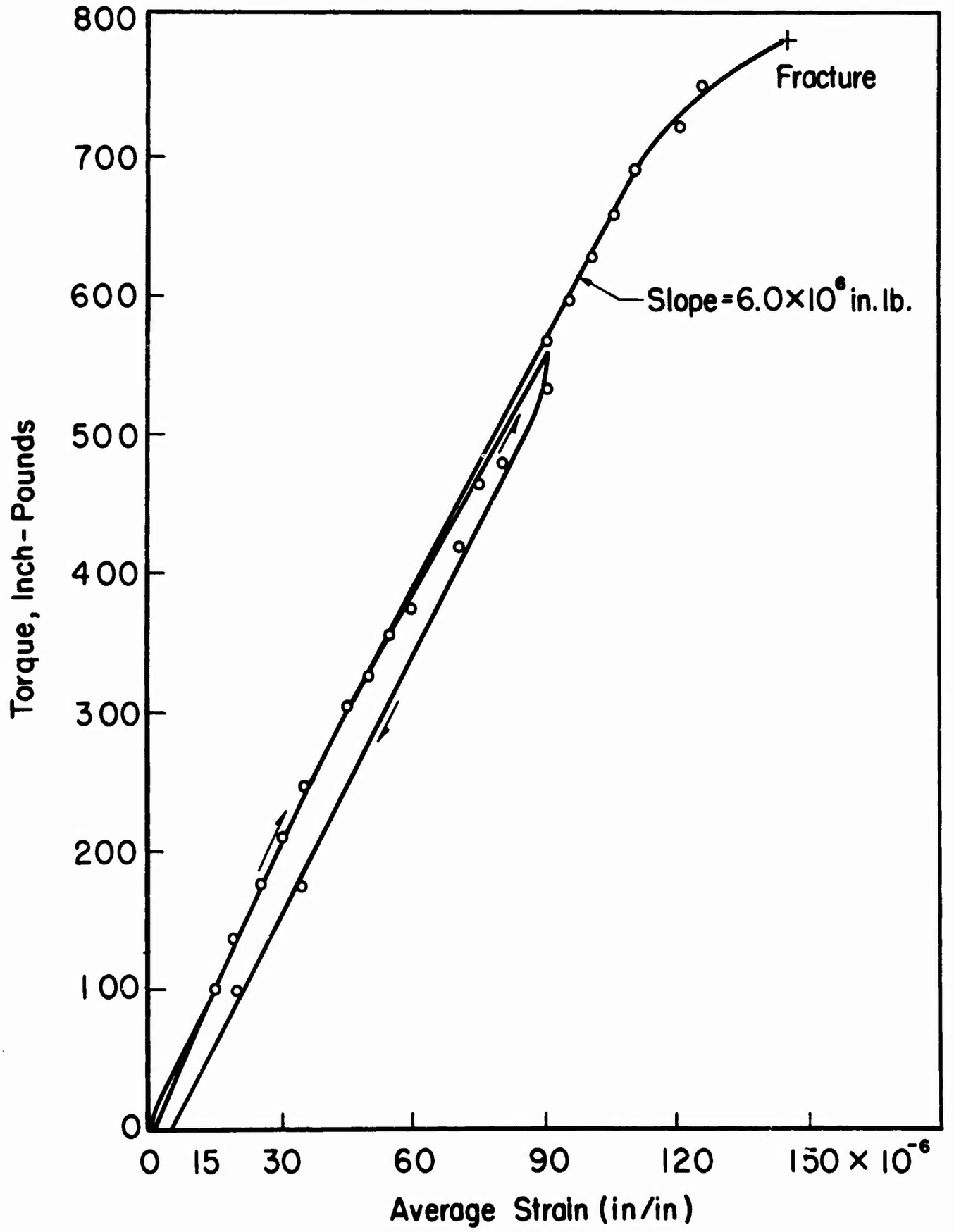

Figure 32. Results of Torsion Experiment on Granite

For the specimen used in this test, R_1 = 1.023 inches and R_2 = 0.773 inch. Therefore,

$$\tau = \frac{(2)\ (1.023)\ T}{\pi\ (1.097 - 0.357)} = 0.88\ T$$

where τ is in pounds per square inch and T is in inch-pounds.

From Mohr's circle, the shear strain is equal to twice the principal strain. Therefore, the shearing modulus, G , of the rock is found by taking the slope of the T versus $\bar{\varepsilon}$ curve and multiplying it by 0.88/2 or 0.44 psi per inch-pound.

The slope of the T versus $\bar{\varepsilon}$ is 6×10^6 inch-pound. Therefore, the torsional stiffness is

$$G = (6 \times 10^6 \text{ in.-lb})\ (0.44 \text{ lb/in.}^2\text{/in.-lb})$$

$$G = 2.64 \times 10^6 \text{ psi}$$

This value may be compared with the results from uniaxial experiments by using formula (1) of Section II. Using the nominal measured values for the material we have

$$E = 8.0 \times 10^6 \text{ psi}$$

$$\nu = 0.275$$

$$G = \frac{E}{2(1 + \nu)} = 3.13 \times 10^6 \text{ psi}$$

which is reasonable agreement between the two methods considering the anisotropic nature of the material, as discussed in Section II.

Figure 32 indicates that the torsion experiment was continued until fracture occurred. A photograph of the failed specimen is presented in figure 33.

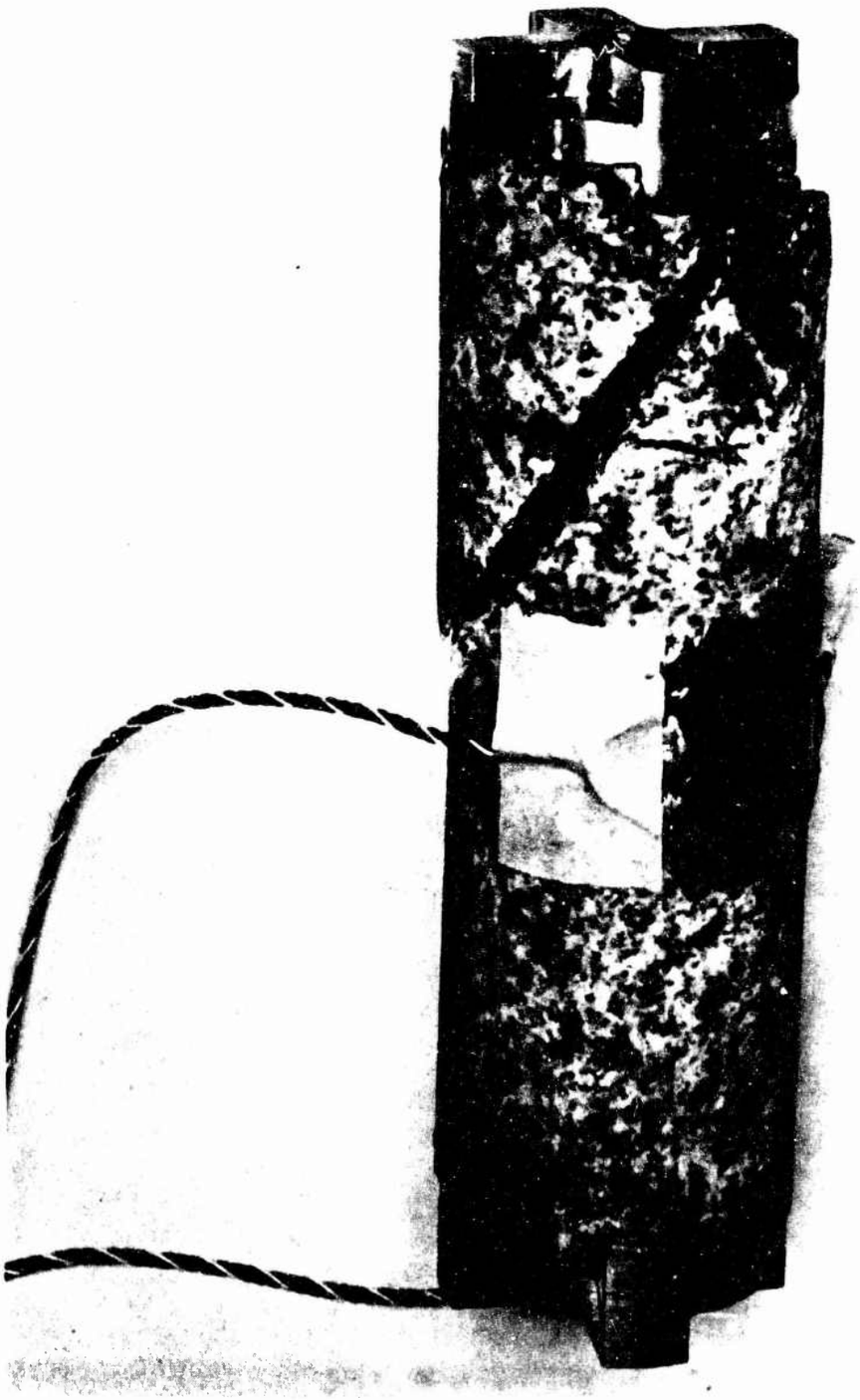

Figure 33. Fractured Torsion Specimen

SECTION VI

50 KILOBAR SYSTEM

The purpose of this chapter is to discuss and present plans of a solid and liquid pressurization system of 50 kilobars designed to accept 1-1/2 inch diameter specimens.

1. Solid System

Figure 34 shows the basic unit. In essence, it closely resembles the one designed by Daniels and Jones.[31] The main parts are the multiring vessel with a carbide core and two steel-sheathed carbide anvils. This type of vessel employs a crushable gasket. Teflon is recommended. One of the authors (L. A. Finlayson) has built and made pressure runs with such a design with a 1/2 inch bore. By enlarging everything to give a bore size of 1-5/8 inch, to accommodate a 1-1/2 inch specimen, the load to achieve 50 Kb would be approximately 1100 tons.

Compressibility data would be obtained by anvil displacement versus load (or pressure). The values generated would be compared with those of known substances. The pressure medium could be silver chloride, cesium chloride, prophylite or any suitable combination of these. Triaxial loading under high hydrostatic pressures could be obtained by adjusting the length of the specimen so that the anvil would contact the specimen at various pressure levels.

Instrumentation for this type of system would include pressure calibration circuitry (Bismuth I-II phase transition) and thermocouple wiring for monitoring temperatures and heating current. This type of anvil may be used to above 2000 degrees C. High temperatures could be obtained by passing high current at low voltage through the carbide anvils or piston and a heater tube surrounding the specimen. Heater tube material could be platinum, graphite or nickel.

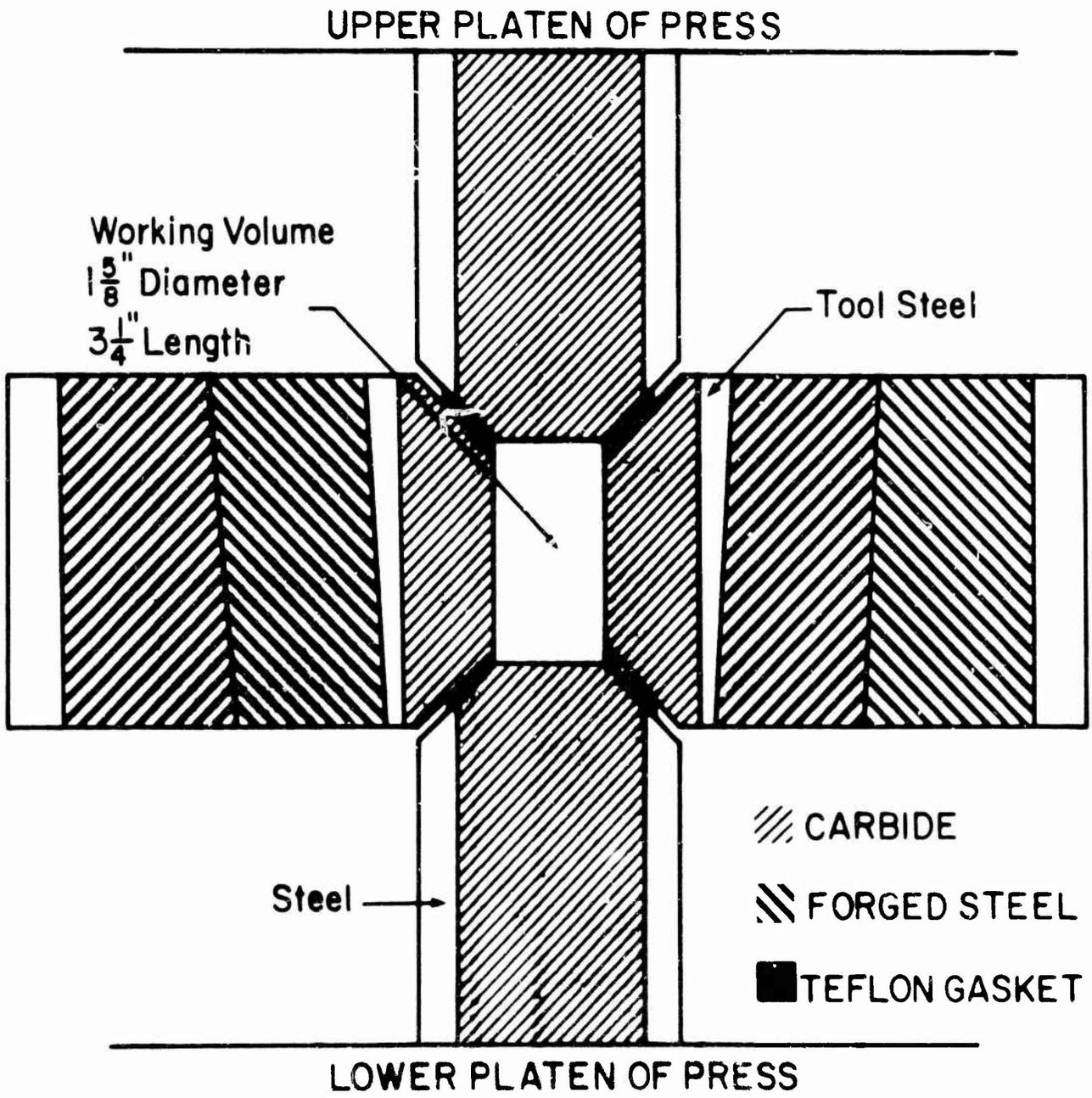

Figure 34. Schematic Diagram of 50 Kilobar Solid System

2. Liquid System

Figure 35 shows the basic unit. The vessel consists of a center core with a bore of 1-5/8 inch diameter. This core is held under compression by a multiring configuration as shown. The multiring unit can be forced upward on the taper, thereby increasing the compressive confining stresses as higher pressures are reached. This minimizes the bore deformation. The upper plug and piston (carbide) are stroked downward to achieve the 50 Kb pressure. The force to move this piston downward would come from a cylinder and piston mounted above the 50 Kb unit. The pressure here would be piped in from a separate pump. Pressure and bore size could range from 10Kb and a 3-3/4 inch piston to 5 Kb and a 5-1/4 inch piston. The choice would be dictated by pump availability.

Electrical leads would be brought in through the bottom seal plug. The bottom seal plug would be restrained from downward force by being blocked to the bottom press platen.

The pressure vessel instrumentation would be similar to that of the solid system. Specimen instrumentation would be possible with a liquid system, whereas with the solid system it is difficult to imagine a suitable technique.

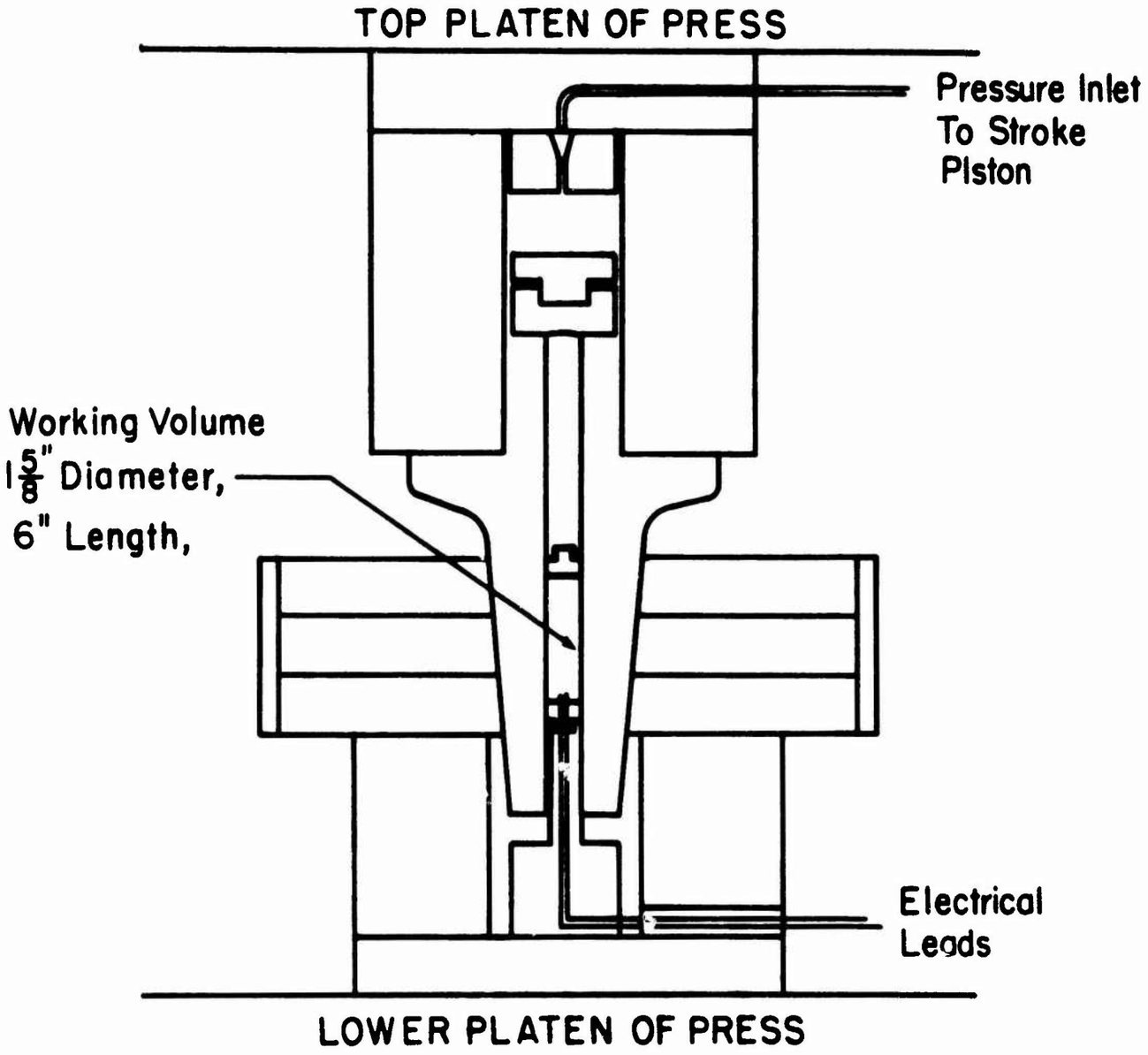

Figure 35. Schematic Diagram of 50 Kilobar Liquid System

SECTION VII

CONCLUSIONS AND RECOMMENDATIONS FOR FUTURE EFFORTS

It has been shown that (1) large samples of geologic materials can be subjected to liquid pressures of the order of kilobars, (2) that materials such as soil can be encapsulated so as to prevent the intrusion of high pressure fluids and (3) that the deformations of highly deformable materials, such as soil, can be measured in a high pressure environment.

Although each of these, and the other techniques developed in this study, are significant and important, they have limitations. Some of the limitations are obvious to the reader, as, for example, the fact that 10 kilobars pressure was not reached with the particular pump-intensifier-large vessel combination, or the inability of the copper encapsulants to withstand pressures greater than 25,000 psi when used on Ottawa sand. Other features of the techniques developed in this study, both good and bad, are not obvious unless one has been intimately involved in the investigation. Therefore, it is felt that this section can be utilized most advantageously by presenting an objective evaluation of the equipment and techniques so that the study will be of maximum benefit to others contemplating investigations of a similar nature.

For ease of reading and future reference the section will be divided so as to concentrate attention on one facet of the investigation at a time. The order of presentation will, more or less, follow the order in which the equipment and techniques were presented in Section IV. When appropriate, the facilities and their suggested refinements will be discussed according to whether tests are to be done on soil or on rock.

1. Stress Application

a. Generation of Pressure in a Large-Capacity Vessel

As mentioned earlier, it was impossible to reach 10 kilobars pressure in the vessel with the pressure generating system which incorporated the differential area pressure intensifier. There was nothing, theoretically, wrong with the intensifier because, if the vessel was shut off from the system, it was a relatively simple matter to raise the pressure in the remainder of the system to 100,000 psi, which was the limit of the Heise gage. Presumably, had the system, with the vessel excluded, contained a pressure transducer suitable for pressures greater than 100,000 psi (the calibrated manganin coil was inside the vessel) it would have been possible to reach 150,000 psi.

The reason that it was possible to generate these high pressures is because of the small volume of oil in the system when the vessel is excluded. Only one stroke of the intensifier's piston is required for raising the pressure up to 100,000 or more psi. However, when the vessel is included, with its working volume of some 360 cubic inches, the intensifier must be repeatedly stroked to reach the higher pressure levels. It is during this repeated stroking that damage occurs to the seals around the piston. The seals then leak and the test has to be terminated to repair the intensifier.

This reoccurring problem with the intensifier led to the decision to build a pump suitable for generating 150,000 psi fluid pressures. The pump is designed after the one described by Whalley and Lavergne.[31]

Unfortunately, as described in Section IV, the highest pressure obtained with this type of pressure-generating system was 87,000 psi. It appears that the use of such a pump is limited to vessels of rather small volume.

It is recommended that a pressure-generating system for large capacity vessels incorporate an intensifer which is of sufficient size so that only one stroke of the piston is required to raise the pressure from that obtained by a commercially available pump (such as the Haskel) to the maximum pressure required. This would eliminate the need of repeatedly stroking the piston of the intensifier and, therefore, minimize the possibility of damaging the high pressure seals around the piston.

b. Volumetric and Linear Compressibility Tests

The bulk compressibility apparatus proved to be a suitable device for measuring the bulk properties of geologic materials. It has the distinct advantage that it provides a means of determining the bulk compressibility of materials such as soils. However, discretion must be exercised when deciding how to make the measurements so as to obtain suitable accuracy. That is, based on the desired accuracy one must decide whether to measure the absolute compressibility, as done here with the sand and clay, or measure it relative to a material of known compressibility, as done with the diorite.

The importance of choosing the proper technique is apparent from consideration of the two methods. When the compressibility of a material is measured relative to a known material one does not have to be concerned with either the compressibility or the amount of fluid necessary to fill the remaining volume in each chamber. This, then, removes two sources of error which could significantly influence the accuracy of the data obtained on materials of relatively low (relative to the oil) compressibility. However, for materials which undergo appreciable volume changes under pressure, such as unsaturated soils, sufficient accuracy is obtained by measuring the absolute compressibility of the material. Here, the errors mentioned before will add only a small error to the measurement because of the relatively high compressibility of the soil.

For anisotropic materials it is frequently desirable to know the linear compressibilities. This requires that the strains be obtained in three orthogonal directions as the sample is subjected to a state of hydrostatic stress. Obviously, the bulk compressibility apparatus is not suitable for these measurements. They could be obtained, however, by using an apparatus similar to that of the confined compression fixture, instrumented with two orthogonal horizontal slidewires in addition to the axial slidewires. A simpler technique, suitable for measuring the linear compressibility of rocks, is to affix strain gages to 3 mutually perpendicular faces of a cube-shaped specimen.

c. Uniaxial and Confined Compression Tests

The confined compression apparatus provided a suitable means for subjecting relatively large rock and soil specimens to a stress difference in a high pressure environment. Although the fixture proved beneficial in this study, certain considerations of its general applicability are appropriate.

In determining the mechanical properties of rock, particularly values of strength, it is extremely important that the specimen be subjected to a state of uniform stress. One of the most common causes of a non-uniform stress state is bending which is the result of either non-parallelism of the specimens ends or of the platens which contact the specimen. It is suggested, then, that the movable piston, in an apparatus similar to the one used here, have a length equal to at least twice the diameter of the chamber. This would eliminate, to within machining tolerances, the possibility of non-parallelism of the platens. In addition, since the strength of some rock types increases rapidly with pressure, very high axial loads may be required to fracture a specimen. Therefore, when used for strength determinations, the wall thickness of the confined compression apparatus may have to be thicker than that used here to avoid exceeding the yield point of the steel.

One very desirable addition to the apparatus would be a load cell in direct contact with the specimen. This would increase the accuracy of the stress measurements by eliminating the need to correct for frictional force supported by the O-rings of the movable piston. This addition would be particularly worthwhile for tests on soil where, because of its relatively low load-carrying ability, it is important to maximize the sensitivity of the stress measurements.

2. Deformation Measurements

A very significant limitation of past studies was overcome in the development of a slidewire fixture capable of measuring the strains of highly deformable materials. This is felt to be one of the more important contributions of this study.

As described in Section IV, three types of fixtures were fabricated. The use of any one depends upon the particular application. The first type, consisting of bakelite support pads, razor blades and leaf spring was very satisfactory when used where there was no chance of relative movement between the support structure of the fixed blades and the support structure of the movable blade. Its use on the bulk compressibility apparatus, therefore, proved to be an excellent application. In the confined compression experiments,however, where the slidewire fixture had more than one degree of freedom, the movable blade would occasionally loose contact with the slidewire. In addition, its fabrication was rather time-consuming and it was thought that a more expendable slidewire would be more suitable, so that, if a specimen failed and the slidewire fixture were destroyed, replacement would be less costly.

The second and third type of slidewires were designed with these criteria in mind. They were relatively easy to fabricate and the wire was constrained sufficiently so that it would maintain contact with the points at which the voltage was to be measured.

The second type, illustrated shcematically in figure 18, was found to be too delicate. Of particular trouble were the several points at which the slidewire itself was joined to either the voltage leads or the tensioning springs.

The third type, shown in figure 19, appears to offer a solution to the majority of prior difficulties. Its fabrication is not difficult and the movable brass screw is constrained so as to remain in contact with the slidewire. This system was used during the confined compression test on Ottawa sand to 25,000 psi and provided data from which the axial strains were calculated. One problem which was discovered when it was subjected to about 60,000 psi was that the Plexiglas cracked around the sites of the brass screws. Presumably this is due to th difference in compressibility of the two materials.

So even this design requires further refinements. However, it is felt that the majority of the difficulties associated with measuring large deformations have been overcome.

3. Specimen Encapsulation

Several different types of encapsulants were used in this study. Their suitability will be discussed briefly with suggestions for further improvements.

The silicone rubber (RTV-102, General Electric) has been found to be an excellent jacketing material in a high pressure environment when the liquid is either kerosene or hydraulic oil.[2] However, its use is not recommended when using silicone oil as the rubber tends to decompose and eventually leak.

The encapsulation of the sand and clay specimens with copper foil proved to be a suitable technique, particularly for dry specimens. The technique was, to a certain extent, undependable when encapsulating saturated or nearly-saturated specimens because of the difficulty of soldering the cover on without creating any steam.

Another disadvantage of the copper containers was the soldered seam running up one side of the can. Both these difficulties could be avoided by using seamless aluminum beverage cans which can be closed with a commercially available canning tool.

It is desirable that the jacketing material be as weak and flexible as possible so as not to support any of the stress state applied to the specimen, yet be strong enough to prevent the intrusion of the high pressure fluid. As higher pressure levels are reached the thickness of the jacketing must be increased. It would appear that the load carrying ability of the jacketing should be determined so that one could decide exactly what contribution it makes toward supporting the applied stresses.

REFERENCES

1. Brace, W. F., "Brittle Fracture of Rocks," State of Stress in the Earth's Crust, New York, Elsevier, 732 pp., 1964.

2. Paulding, B. W., "Crack Growth During Brittle Fracture in Compression," Ph. D. Thesis, Massachusetts Institute of Technology, June 1965.

3. Lisowski, A., "Failure of Rock Cubic Specimens in the Light of the Theory of Elasticity," Acad. Polonaise Sci. Bull., Ser. Sci. Tech., Vol. 7, No. 5, p. 341-351, 1959.

4. Filon, L. N. G., "On the Elastic Equilibrium of Circular Cylinders Under Certain Practical Systems of Loads," Phil. Trans. A., Vol. 198, p. 147-233, 1902.

5. Birch, Francis, "The Velocity of Compressional Waves in Rocks to 10 Kilobars, Part 2," Jour. Geop. Res., 66, p. 2199-2224, 1961.

6. Brace, W. F., "Some New Measurements to Linear Compressibility of Rocks," Jour. Geop. Res., Vol. 70, No. 2, January 15, 1965, pp. 391-398.

7. Walsh, J. B., "The Effect of Cracks on the Compressibility of Rock," Jour. Geop. Res., 70, p. 381-389, 1965.

8. Voight, W., Lehrbuch der Kristallphysik, B.G. Terebner, Leipzig, 1928.

9. Reuss, A., "Berechnung Der Fleissgrenze Von Mischkristallen Auf Grund Plastizitats Bedingung Fur Einkristalle," Z. Angew Math. U. Meth., Vol 9, p. 49-58, 1929.

10. Walsh, J. B., "The Effect of Cracks on the Uniaxial Elastic Compression of Rocks," Jour. Geop. Res., 70, p. 399-411, 1965.

11. Ide, J. M., "Comparison of Statically and Dynamically Determined Young's Modulus of Rocks," Proc. Natl. Acad. Sci., U.S., 22, 81-92, 1936.

12. Zisman, W. A., "Comparison of the Statically and Seismically Determined Elastic Constants of Rocks," Proc. Natl. Acad. Sci., U.S.,19, 680-686, 1933.

13. McClintock, F. A. and Walsh, J. B., "Friction of Griffith Cracks in Rocks Under Pressure," Proc. Natl. Congr. Appl. Mech., 4th, Berkeley, 1015-1021, 1962.

14. Griffith, A. A., "The Phenomena of Rupture and Flow in Solids," Phil. Trans. Roy. Soc. London , A., 221, 163-197, 1921.

15. Griffith, A. A., "The Theory of Rupture," Proc. First Int. Cong. Appl. Mech., Delft, 55-63, 1924.

16. Handin, John, personal communication, 1964.

17. Paterson, M. S., "Experimental Deformation and Faulting in Wombeyan Marble," Geol. Soc. Amer. Bull. 69, 465-746, 1958.

18. Jaeger, J. C., "The Frictional Properties of Joints in Rocks," Geofisica pure e applicata, Milano, 43, 148-158, 1959.

19. Jaeger, J. C., Elasticity, Fracture and Flow, New York, John Wiley and Sons, Inc., 208 pp., 1962.

20. Nadai, A., Theory of Flow and Fracture of Solids, New York, McGraw Hill, 1950, 572 pp.

21. Brace, W. F., "An Extension of the Griffith Theory of Fracture Rocks," Jour. Geop. Res., 65, 3477-3480, 1960.

22. Inglis, C. E., "Stresses in a Plate Due to the Presence of Cracks and Sharp Corners," Inst. Naval Arch. (London), 55, 219-230, 1913.

23. Brace, W. F.,"Dependence of Fracture Strength of Rocks on Grain Size," Penn. State Univ. Mineral Expt. Sta. Bull., No. 76, 99-103, 1961.

24. Walsh, J. B. and Brace, W. F., "A Fracture Criterion for Brittle Anisotropic Rock," Jour. Geop. Res., 69, 3449-3456, 1964.

25. Donath, F. A., "Experimental Study of Shear Failure in Anisotropic Rocks," Geol. Soc. Amer. Bull., 72, 985-990, 1961.

26. Cornish, R. H. and Ruoff, A. L., "Electrical Leads for Pressure Vessels to 30 Kilobars," Review of Scientific Instruments, Vol. 32, No. 6, June 1961, pp. 639-641.

27. Gerdeen, J. C., "Effects of Pressure on Small Foil Strain Gages," Experimental Mechanics, Vol. 3, No. 3, March 1963, pp. 73-80.

28. Milligan, R. V., "The Effects of High Pressure on Foil Strain Gages," Experimental Mechanics, Vol. 4, No. 4, February 1964, pp. 25-36.

29. Brace, W. F., "Effect of Pressure on Electric-Resistance Strain Gages," Experimental Mechanics, Vol. 4, No. 7, July 1964, pp. 212-216.

30. Milligan, R. V., "The Effects of High Pressure on Foil Strain Gages on Convex and Concave Surfaces," Experimental Mechanics, Vol. 5, No. 2, February 1965, pp. 59-64.

31. Whalley, E. and Lavergne, A., "Automatic Air-Driven Oil Pump for 10 Kilobars," Review of Sci Instruments, Vol. 32, No. 9, pp.1062-1063, 1961.

32. Daniels and Jones, "Simple Apparatus for the Generation of Pressures Above 100,000 Atmospheres Simultaneously with Temperatures Above 3000°C," Rev. Sci. Instr., Vol. 32, No. 8, 1961.

Unclassified
Security Classification

DOCUMENT CONTROL DATA - R&D

(Security classification of title, body of abstract and indexing annotation must be entered when the overall report is classified)

1. ORIGINATING ACTIVITY (Corporate author) IIT Research Institute Chicago, Illinois	2a. REPORT SECURITY CLASSIFICATION Unclassified 2b GROUP

3. REPORT TITLE

BEHAVIOR OF ROCKS AND SOILS UNDER HIGH PRESSURE

4. DESCRIPTIVE NOTES (Type of report and inclusive dates)

Final Report 1 June 1964 to 1 August 1965

5. AUTHOR(S) (Last name, first name, initial)

Paulding, B. W.; Cornish, R. H.; Abbott, B. W.; Finlayson, L. A.

6. REPORT DATE	7a. TOTAL NO. OF PAGES	7b. NO. OF REFS
December 1965	106	32

8a. CONTRACT OR GRANT NO.	9a. ORIGINATOR'S REPORT NUMBER(S)
AF29(601)-6411 b. PROJECT NO. 5710 Subtask: 13.144 c. d.	AFWL-TR-65-51 9b. OTHER REPORT NO(S) (Any other numbers that may be assigned this report) IITRI Project No. M6083

10. AVAILABILITY/LIMITATION NOTICES

Distribution of this document is unlimited.

11. SUPPLEMENTARY NOTES	12. SPONSORING MILITARY ACTIVITY
	Air Force Weapons Laboratory (WLDC) Kirtland AFB, New Mexico 87117

13. ABSTRACT

This report describes a program which was directed toward developing a capability suitable for generating engineering data on the high pressure mechanical properties of geologic materials. To provide the greatest possible contribution this effort concentrated on three of the most important deficiencies in high pressure experimental technology: (1) development of a system capable of accepting relatively large samples so that more-nearly representative data may be obtained than with the smaller samples used previously, (2) development of a system suitable for monitoring the strains of highly deformable geologic materials, and (3) development of an encapsulating technique for soils. Each of these objectives was attained to a certain degree. Specimens up to three inches in diameter were subjected to fluid pressures of several kilobars. The deformation of soil was measured with a potentiometric slidewire device. An encapsulating technique was developed for soils which was suitable up to about two kilobars. Further refinements are necessary, but it appears that the more important of the limitations of past studies have been overcome.

DD FORM 1 JAN 64 1473

Unclassified
Security Classification

Unclassified
Security Classification

14. KEY WORDS	LINK A		LINK B		LINK C	
	ROLE	WT	ROLE	WT	ROLE	WT
Rock Mechanics						
Soil Mechanics						
Testing under high pressure						
Bulk Compressibility						
Uniaxial Compression						
Confined Compression						
Torsion						
Strain Gage Instrumentation						
Slidewire Instrumentation						
Soil Encapsulation						

INSTRUCTIONS

1. ORIGINATING ACTIVITY: Enter the name and address of the contractor, subcontractor, grantee, Department of Defense activity or other organization *(corporate author)* issuing the report.

2a. REPORT SECURITY CLASSIFICATION: Enter the overall security classification of the report. Indicate whether "Restricted Data" is included. Marking is to be in accordance with appropriate security regulations.

2b. GROUP: Automatic downgrading is specified in DoD Directive 5200.10 and Armed Forces Industrial Manual. Enter the group number. Also, when applicable, show that optional markings have been used for Group 3 and Group 4 as authorized.

3. REPORT TITLE: Enter the complete report title in all capital letters. Titles in all cases should be unclassified. If a meaningful title cannot be selected without classification, show title classification in all capitals in parenthesis immediately following the title.

4. DESCRIPTIVE NOTES: If appropriate, enter the type of report, e.g., interim, progress, summary, annual, or final. Give the inclusive dates when a specific reporting period is covered.

5. AUTHOR(S): Enter the name(s) of author(s) as shown on or in the report. Enter last name, first name, middle initial. If military, show rank and branch of service. The name of the principal author is an absolute minimum requirement.

6. REPORT DATE: Enter the date of the report as day, month, year, or month, year. If more than one date appears on the report, use date of publication.

7a. TOTAL NUMBER OF PAGES: The total page count should follow normal pagination procedures, i.e., enter the number of pages containing information.

7b. NUMBER OF REFERENCES: Enter the total number of references cited in the report.

8a. CONTRACT OR GRANT NUMBER: If appropriate, enter the applicable number of the contract or grant under which the report was written.

8b, 8c, & 8d. PROJECT NUMBER: Enter the appropriate military department identification, such as project number, subproject number, system numbers, task number, etc.

9a. ORIGINATOR'S REPORT NUMBER(S): Enter the official report number by which the document will be identified and controlled by the originating activity. This number must be unique to this report.

9b. OTHER REPORT NUMBER(S): If the report has been assigned any other report numbers *(either by the originator or by the sponsor)*, also enter this number(s).

10. AVAILABILITY/LIMITATION NOTICES: Enter any limitations on further dissemination of the report, other than those imposed by security classification, using standard statements such as:

(1) "Qualified requesters may obtain copies of this report from DDC."

(2) "Foreign announcement and dissemination of this report by DDC is not authorized."

(3) "U. S. Government agencies may obtain copies of this report directly from DDC. Other qualified DDC users shall request through _____."

(4) "U. S. military agencies may obtain copies of this report directly from DDC. Other qualified users shall request through _____."

(5) "All distribution of this report is controlled. Qualified DDC users shall request through _____."

If the report has been furnished to the Office of Technical Services, Department of Commerce, for sale to the public, indicate this fact and enter the price, if known.

11. SUPPLEMENTARY NOTES: Use for additional explanatory notes.

12. SPONSORING MILITARY ACTIVITY: Enter the name of the departmental project office or laboratory sponsoring *(paying for)* the research and development. Include address.

13. ABSTRACT: Enter an abstract giving a brief and factual summary of the document indicative of the report, even though it may also appear elsewhere in the body of the technical report. If additional space is required, a continuation sheet shall be attached.

It is highly desirable that the abstract of classified reports be unclassified. Each paragraph of the abstract shall end with an indication of the military security classification of the information in the paragraph, represented as *(TS)*, *(S)*, *(C)*, or *(U)*.

There is no limitation on the length of the abstract. However, the suggested length is from 150 to 225 words.

14. KEY WORDS: Key words are technically meaningful terms or short phrases that characterize a report and may be used as index entries for cataloging the report. Key words must be selected so that no security classification is required. Identifiers, such as equipment model designation, trade name, military project code name, geographic location, may be used as key words but will be followed by an indication of technical context. The assignment of links, rules, and weights is optional.

Unclassified
Security Classification